Bioinspiration &
Biomimetics

TOPICAL REVIEW • OPEN ACCESS

Designing McKibben muscles: a critical review for practical implementation

To cite this article: V G Kortman *et al* 2026 *Bioinspir. Biomim.* **21** 031002

Bioinspiration & Biomimetics

Check for updates

OPEN ACCESS

RECEIVED
20 October 2025

REVISED
13 April 2026

ACCEPTED FOR PUBLICATION
29 April 2026

PUBLISHED
18 May 2026

TOPICAL REVIEW

Designing McKibben muscles: a critical review for practical implementation

V G Kortman[1,2,*], J Jovanova[2], H Nabae[3], G Endo[3], K Suzumori[3] and A Sakes[1]

1 Department of BioMechanical Engineering, Delft University of Technology, Mekelweg 2, Delft 2628CD, The Netherlands
2 Department of Maritime and Transport Technology, Delft University of Technology, Mekelweg 2, Delft 2628CD, The Netherlands
3 Suzumori-Endo Lab, Institute of Science Tokyo, 2-12-1 Ookayama, Meguro-ku, Tokyo, Japan
* Author to whom any correspondence should be addressed.

E-mail: v.g.kortman@tudelft.nl

Keywords: artificial muscles, McKibben Muscles, soft robotics, bio-inspired design, actuator

Abstract

McKibben artificial muscles (AMs) are known as a prominent class of pneumatic actuators in soft robotics and biomechanical engineering, due to their unique structure and multifunctionality. This paper presents a comprehensive review of recent advancements in McKibben AMs, focusing on their performance, structural variations, and operational principles. A systematic literature search on Scopus identified 146 relevant articles, which were analysed for both performance metrics and design characteristics. Inspired by natural muscle behaviour, McKibben AMs enable complex motions such as bending, linear extension, and twisting. These actuators can be organised as individual or bundled systems: individual units are typically arranged in linear or circular patterns, while bundled systems occur in serial, parallel, braided, convergent, or pennate configurations. Recent innovations in smart actuation methods, braided sleeves and internal bladders have expanded their capabilities, enabling embedded sensing, environmental adaptability and untethered operation. Additionally, alternative manufacturing methods offer promising solutions for developing McKibben muscles with enhanced functionality and tailored properties.

1. Introduction

In the domain of soft robotics and biomechanical engineering, McKibben artificial muscles (AMs) have emerged as a notable class of pneumatic actuators, characterised by their unique structural composition and versatile functionality. Positioned at the intersection of engineering and biology, McKibben AMs are conceived as a means to imitate natural musculature. Developed by J.L. McKibben in the late 1950s, these AMs illustrate inherent compliance, low mass, and controllability which render them particularly suitable to a spectrum of applications, such as wearables, robotics, prosthetics, and rehabilitation engineering.

The typical composition of a McKibben AM involves a flexible outer sleeve, usually a braid or textile, commonly crafted from materials such as nylon or polyethylene, providing the necessary structural integrity. Enveloped within this outer sleeve is an inner pneumatic bladder, typically composed of a compliant material, such as latex, rubber, or silicone, see figure 1. At the distal tip of the McKibben AM, an end cap is placed to close off the pneumatic bladder. The synergy between the flexible outer sleeve and the inflatable inner bladder enables controlled, biomimetic motion of the McKibben AM, similar to natural muscles. To activate the muscle, pressurised fluid is normally injected into the open end of the inner pneumatic bladder using a connection cap. Once the inner bladder is fully pressurised, the volume of the inner bladder increases and produces a force in the radial direction against the braided sleeve. The braided sleeve subsequently transforms the generated radial force into the length direction along the braid axis [1].

McKibben AMs exist in a large size-range from approximately 1 mm to 50 mm in diameter and variable lengths. For example, a McKibben AM with a diameter of 1.5 mm was developed by De Volder *et al* [2] that could achieve contraction forces of 6 N, an axial strain of 15%, and a maximal actuation speed of 350 mm s^{-1}, whereas a much larger hydraulic AM

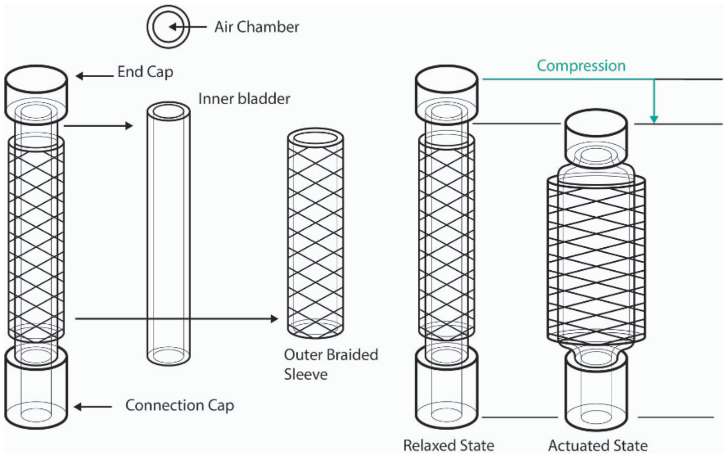

Figure 1. Structural composition of McKibben artificial muscles (AMs). McKibben AMs comprise of a flexible outer braided sleeve, an inner air chamber, an end cap, and a connection cap. By inflating the inner pneumatic bladder, the McKibben AM will either expand or compress, depending on the braiding angle.

was developed by Mori *et al* [3], with a diameter of 40 mm that could achieve up to 28 kN. State-of-the art McKibben AMs can generate axial strains of up to 30%–35% [4].

McKibben AMs have recently regained significant attention as soft robotic systems increasingly demand lightweight, high-compliance, and high-force actuators. At the same time, research on McKibben AMs has become widely scattered across biomechanics, robotics, materials science, and rehabilitation engineering journals, making it difficult for new researchers to navigate the field. Therefore, this paper undertakes a comprehensive review to illustrate the intricate mechanical principles governing McKibben AMs and explores their diverse configurations across disciplines. By summarising how key design and performance parameters influence actuator behaviour, this work aims to provide clear, implementation-oriented guidance and fill a gap in literature for researchers who seek an overview. For this purpose, we have conducted a literature review in Scopus (05-02-2024) using 'McKibben' as the single keyword, which yielded 838 results. Papers focusing on analytical and experimental studies involving McKibben AM were included in this study, resulting in a total of 146 included articles. Review papers and papers solely focusing on control, finite element analysis, the application of McKibben AMs in other structures, and artificial intelligence, as well as non-English papers were excluded from this review. Generally, closed-loop PID-based force or position control remains the most commonly applied approach for McKibben actuators [5, 6]. For comprehensive treatments of control design and system dynamics, we refer readers to Tondu & Lopez [5], Caldwell *et al* [6], and De Volder *et al* [2].

We focus on classical McKibben AMs as their architecture, fabrication methods and design parameters form a distinct class of pneumatic AMs with well-defined characteristics and industrially scalable fabrication. Including other pneumatic artificial actuators, such as fibre-reinforced elastomer actuators, would substantially broaden the scope and reduce the focus of the study.

2. McKibben performance characteristics

2.1. Force and contraction characteristics

Figure 2 shows the composition and geometric variables of McKibben AMs. McKibben AMs are often characterised based on their tension force, contraction force, and blocking force. The tension force is the force generated along the wires in the outer sleeve when the McKibben is pressurised, whereas the contraction force is the force produced during muscle contraction. The contraction force is highest when the axial strain is lowest and varies with the initial braid angle, see figure 3. The blocking force is the resisting force against further contraction when the muscle is pressurised but prevented from shortening. The blocking force opposes the contraction force and, therefore, benefits from friction, whereas the contraction force is negatively affected by friction.

McKibben AMs generate an axial contraction force that can be expressed by the classical Chou & Hannaford model, shown in equation (1), which assumes inextensible fibres and relates the force to the geometry of the actuator [7]. This formulation is widely used in analytical and experimental studies of pneumatic AMs. The same model can also be rearranged into strain-based forms, in which the geometry is expressed as a function of axial strain (ε) [4, 5, 8],

$$F_c = \frac{\pi}{4} \mathrm{PD}_0^2 \left(3\cos^2\theta - 1\right) \tag{1}$$

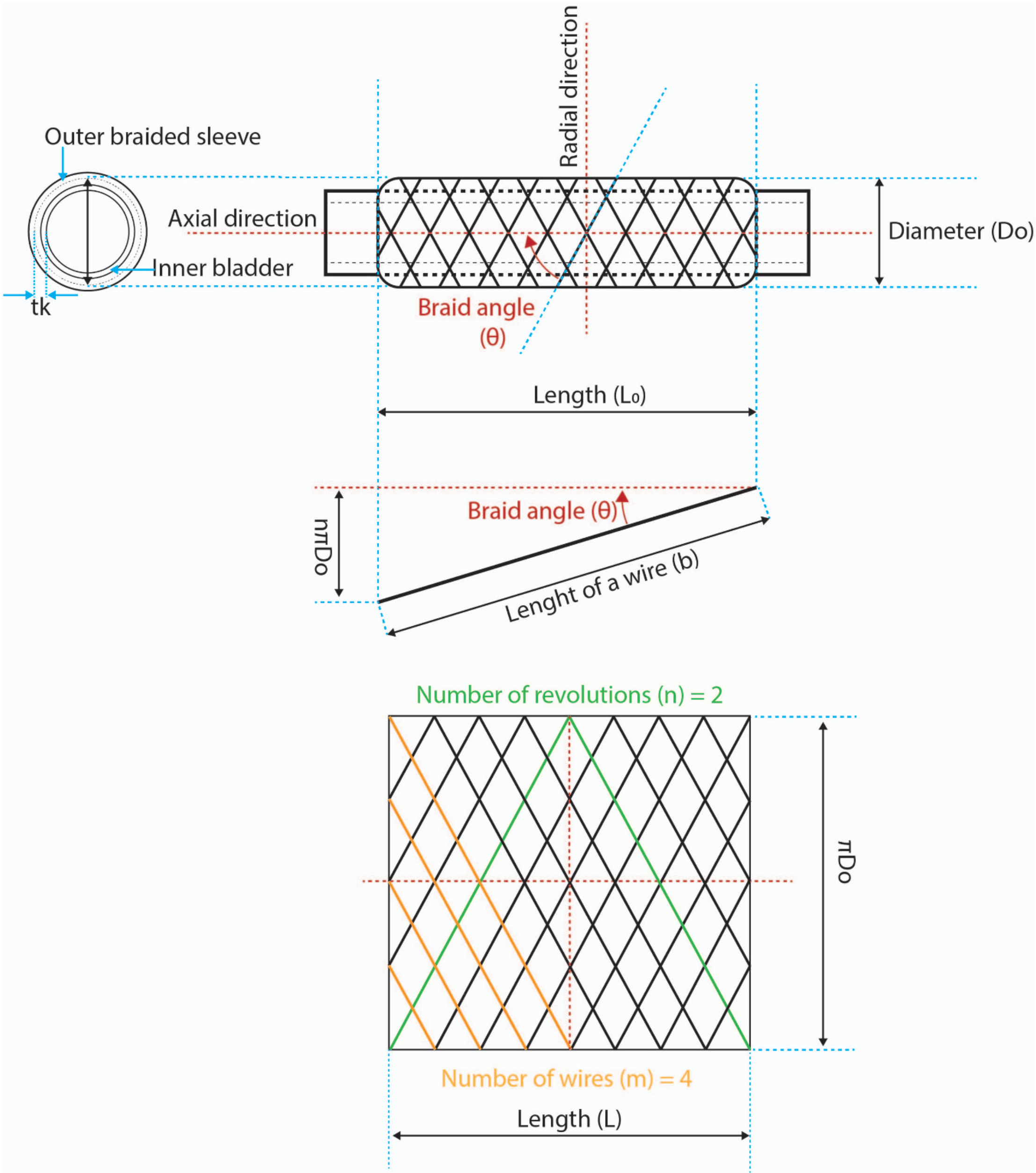

Figure 2. Composition and geometric variables of McKibben artificial muscles (AMs). McKibben AMs composition indicating the sum of the thickness of the bladder with half of the sleeve width (t_k), the braid angle (θ), the initial length of the muscle (L_0), the length of an individual wire (b), the diameter of the McKibben AM (D_0), the number of full rotations per wire (n), and the number of wires in the outer braided sleeve (m).

D_0, P and θ denote the diametric constrant of the AM [mm], the applied pressure [Pa] and the braid angle (defined as the angle between any wire of the outer braid and the axial axis, see figure 2) [°], respectively. Using the inextensible fibre assumption, the diameter of the AM is defined as:

$$D = \frac{b \sin\theta}{n\pi} \quad (2)$$

where b is the length of an individual wire [mm] in the outer braided sleeve and n is the number of full rotations per wire [-], see figure 2.

The axial strain ε is defined as (3), With L_0 the initial length of the McKibben AM [mm] and L the contracted length [mm].

$$\varepsilon = \frac{L_0 - L}{L_0}. \quad (3)$$

The generated contraction force is proportional to the applied pressure, substantiating that McKibben AMs using liquids instead of air, can generate larger amounts of force than those actuated by air [9–15]. Iwata *et al* [9] developed a hydraulic McKibben AM (Ø 21 mm) capable of generating a contraction force of 8 kN. Mori *et al* [3] developed a similar McKibben AM (Ø 40 mm) that could achieve a contraction force of 28 kN by applying high tensile force sleeve wires, optimising the weaving pattern of the outer

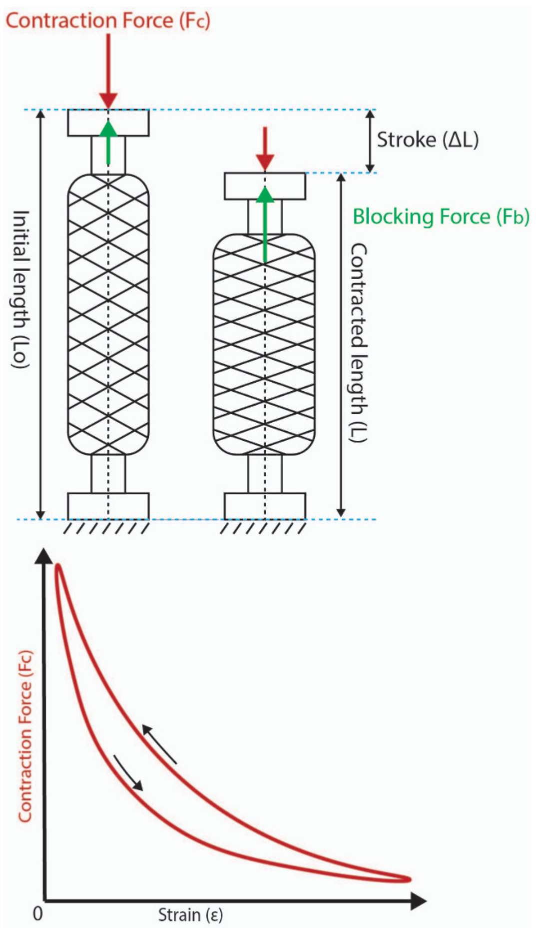

Figure 3. McKibben artificial muscles (AM) performance variables. McKibben AM performance variables indicating the initial length (L_0), contracted length (L), strain (ΔL), axial strain (ε), contraction force (F_c) and blocking force (F_b) of the artificial muscle. The contraction force scales with the contraction ratio, with the maximum contraction force at zero contraction, whereas the blocking force is maximum and full contraction. Hysteresis in the system creates the distinct force loop during inflation and deflation.

braided sleeve, and increasing the strength of the connection and end caps. In the study of Thomalla and Van De Ven [8], a new model was developed for hydraulic McKibben AMs that tracked the generated axial force of the actuator while considering the change in actuator wall thickness. This new model showed increased accuracy of approximately 1% over the state-of-the-art (elastic) force models.

The contraction force is proportional to the outer diameter of the McKibben AM, with larger McKibben AMs able to achieve higher contraction forces, as can be observed from equation (1). The effect of scaling on the performance of McKibben AMs was investigated in more detail in an experimental study by Peel *et al* [14]. It was found that a longer actuator resulted in a larger contraction stroke and lower contraction force. Though contraction forces decreased as the diameter and length decreased, which is in line with equation (1), the force per unit AM volume was shown to increase with decreasing diameter. However, the relative work per actuation volume was decreased by roughly 35% in smaller AMs [14].

McKibben AMs are commonly modelled or characterised as actuators, but their second role as support structure introduces strain–pressure combinations outside of normal actuation regions. This occurs, for example, when the McKibben AMs are placed in an antagonistic configuration. In the study by Olson *et al* [16] a more complete set of possible strain–pressure combinations for McKibben AMs was investigated, including those of passive or unpressurised actuators, as well as pressurised extension and compression beyond the maximum actuation strain. They demonstrate a trade-off between the maximum axial strain and force required to passively extend the AM, and that stiffer elastomers inner bladders require an increase in actuation pressure without a compensatory increase in maximum achieved force.

Different studies describe the dynamic responses of McKibben AMs for different pressures and frequencies [7, 17, 18]. Wenlin *et al* [19] report that the driving frequency across various applications is generally concentrated within 0.3 Hz. They mention that when the driving frequency exceeds 1 Hz, their AMs cannot be fully inflated and deflated anymore due to the viscoelasticity of the bladder. Experiments show that with increasing driving frequency, the amount of hysteresis of the AM increases. Davis *et al* [18] show that major constraining elements on the AM dynamics is the supply pipe and valve resistance, favouring a minimal amount of pipe connectors and large orifice valves.

A large number of papers describes physical, empirical or experimental models of McKibben AMs [5, 20–33]. In these studies, slight alterations are made to the state-of-the-art in terms of the implementation of a more sophisticated friction modulation, noncylindrical shape, and more accurate braiding representations. These studies will not be discussed in detail.

2.2. Energy dissipation

Although the theoretical contraction force can be calculated by equation (1), it does not consider the hardness of the inner bladder and the frictional forces experienced in the McKibben AM. Whilst these properties are neglectable at larger scales, when downsizing the McKibben AMs, these factors need to be considered. Considering the effect of the bladder thickness and the frictional forces in the sleeve, Chou and Hannaford [7, 34] proposed an improved formula for the relationship between the contraction force F_c and the pressure difference P, including a correction for the bladder thickness:

$$F_c = \frac{\pi}{4} P \left[D_0{}^2 \left\{ 3\cos^2\theta - 1 \right\} \right] + \pi P t_k \left[D_0 \left(2\sin\theta - \frac{1}{\sin\theta} \right) - t_k \right] \quad (4)$$

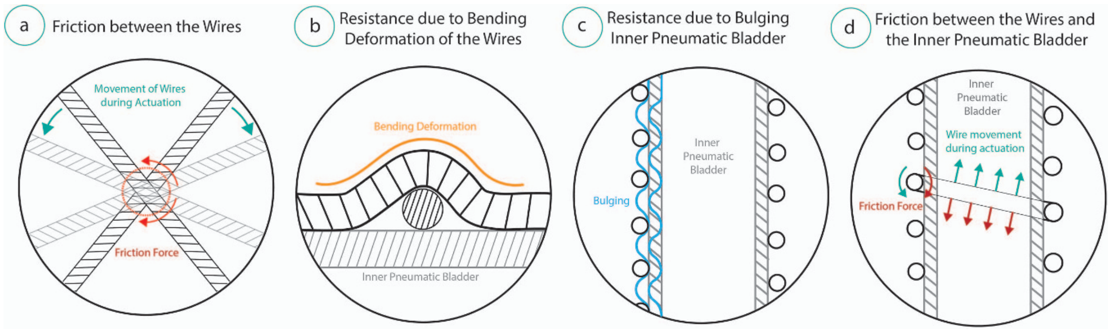

Figure 4. Energy Losses in McKibben artificial muscles. (a) rotational resistance due to the frictional forces between the wires, (b) resistance due to bending deformation of wires, (c) resistance due to bulging of the inner bladder through the sleeve, (d) resistance due to the frictional force between wires and the bladder.

where t_k is the sum of the thickness of the bladder with half of the sleeve width.

However, even though equation (4) represents the characteristics of McKibben AMs more closely than equation (1), there is a substantial gap between experimental data and the predictions due to the lack of considering energy losses in the AM. One of the major energy losses in McKibben AMs is due to frictional resistance and appears as the wires rotate during contraction or extension, see figure 4 [35]. These resistances can be subdivided into:

(1) Rotational resistance due to the frictional forces between wires

During axial contraction or extension, the braiding angle changes as the wires slide over each other. This causes friction, reducing efficiency and increasing hysteresis of the McKibben AM. Efficiency refers to the ratio between the mechanical work delivered during contraction and the pneumatic/hydraulic energy supplied [12]. Surface texture is a key factor influencing wire-to-wire friction. To minimise this friction, a smoother wire surface is more desirable [22], which correlates with the findings of Hoque *et al* [36], as well as less contact points between the wires. If the thickness of the wires or the number of wires is reduced, the maximum axial strain could potentially be improved since the rotational resistance of the threads decreases [35]. Furthermore, to reduce friction further, in some outer sleeves not every wire is woven consistently, with some weaves that are intentionally skipped, thus minimising the rotational resistance of the wires. The number of contact points between the wires can be calculated using the following equation [37]:

$$N_{\text{contact}} = \frac{2b^2 \sin^2\theta \cos^2\theta}{n w_y{}^2}. \qquad (5)$$

With w_y the wire width (mm).

(2) Resistance due to bending deformation of wires

Energy is dissipated in order to produce bending deformation of the wires during movement. Therefore, wires that exhibit lower bending stiffness, such as braided wires or wires out of a more flexible material, can potentially decrease this type of energy loss in the AM.

(3) Resistance due to bulging of the inner bladder through the sleeve

During inflation, the inner bladder will start to expand until it reaches the outer braided sleeve, where the radial expansion is halted and converted into the axial direction. By increasing the applied pressure to the bladder, the bladder can start to bulge through the holes in the outer sleeve, which causes frictional and energy losses, and can lead to rupture. Therefore, there is an interplay between the compliance of the bladder, the elasticity of the bladder material, and the cover factor of the outer braided sleeve.

(4) Resistance due to the frictional force between wires and the bladder

During actuation of the McKibben AMs relative motion between the wires and the bladder ensues. This relative motion results in frictional losses and therefore a loss in efficiency of the McKibben AM.

Taking these factors into account leads to the following equation [35]:

$$F_c = \frac{\pi}{4} \mathrm{PD_0}^2 \left\{ 3\cos^2\theta_0 - 1 \right\} - \frac{4m^2 n}{b \sin\theta_0} \left(M_f + M_d + M_r + M_{tr} \right). \qquad (6)$$

With m is the number of wires in the outer sleeve [−], M_f the resistant moment due to friction between wires [Nmm], M_d the rotational resistant moment due to the bending deformation of wires [Nmm], M_r the rotational resistant moment due to the bulging of the rubber [Nmm], and M_{tr} the resistant moment due to the frictional force between wires and the bladder [Nmm].

As can be seen from equation (6), an increase in the number of wires m in the outer sleeve, reduces the contraction force of the McKibben AM. This is substantiated by the experimental study of Kurumaya *et al* [38], in which they investigated the effect of the inner bladder hardness and number of wires in the outer sleeve on the blocking force and the axial strain of thin McKibben muscles (Ø 1.8 mm). It was found that when the number of outer wires increases, the blocking force also increases due to an increase in friction between the wires, as well as between the wires and the inner pneumatic bladder, at the cost of the axial strain. Additionally, it was found that the number of outer wires need to be at least 24 with a braiding angle of at least 18°, to reduce the risk of rupture. The hardness of the bladder was also found to be an important factor for design because it determines the ease of tube deformation, axial strain, and amount of air pressure required to achieve a given contraction. Davis and Caldwell [39] showed that to determine the number of wires necessary to prevent braid failure of the McKibben AM, the following equation can be used:

$$m = \frac{\mathrm{PD_0}^2\pi\ \cos\theta\ \sin\theta}{2\sigma A_{\mathrm{wire}}}. \tag{7}$$

With *s* representing the ultimate tensile strength of the wire [Pa] and A_{wire} representing the cross-sectional area of the wire [mm^2].

2.3. Fatigue characteristics

When applying McKibben AM in robotic applications, fatigue life is a major challenge. McKibben AMs exhibit fatigue characteristics influenced by the materials used and the cyclic nature of their operation. Over time, repeated inflation and deflation cycles can lead to wear and tear, particularly in the inner bladder and outer braided sleeve, which may result in reduced performance and eventual failure due to material fatigue. In a study of Klute and Hannaford [40], a model was developed that predicts the maximum number of life cycles of a McKibben AM based on available uniaxial tensile properties of the actuator's inner bladder. Experimental results revealed that McKibben AMs fabricated with natural latex rubber bladders have a fatigue limit 24 times greater than actuators fabricated with synthetic silicone rubber at large axial strains. In a study by Wenlin *et al* [19], they found that air leakage in the middle was the most common fatigue phenomenon in their McKibben AM.

2.4. Experimental facilities

Isotonic and isometric testing methods are pivotal in evaluating the performance of McKibben AM. Isotonic testing involves assessing the AM under constant loading conditions, allowing for the measurement of contraction length, contraction force, and speed as the AM performs work against a fixed resistance. This method provides insights into the strain, response time, and mechanical efficiency under dynamic loading scenarios. Conversely, isometric testing measures the AM's force output while maintaining a constant length, thereby evaluating its static force generation capabilities. Together, these methods comprehensively characterise the mechanical properties and functional performance of McKibben AMs.

In a study of Salahuddin *et al* [41], an integrated characterisation method is proposed that combines isometric and isotonic testing. This test set-up allows for simultaneously measuring the free stroke of a McKibben AM, the stroke while operating against an externally applied force (isotonic), the blocked force while keeping the muscle at constant length (isometric); and the force and displacement change when the McKibben AM operates against a return spring (variable force, pressure).

3. McKibben composition characteristics

3.1. Outer sleeve configuration

The outer sleeve of McKibben AMs is normally manufactured using several wires interwoven with each other in a biaxial braiding pattern and fabricated around a mandrel [39, 42]. In biaxial-braided sleeves, a single wire set (generally orientated at an angle in the + and—directions) is interlaced with each other to form the braided fabric surface. Simulations reveal that loads are sustained mostly by the outer braided sleeve, whereas the inner bladder stores the majority of the external work as elastic energy [43]. Geometric variables that affect the final mechanical performance of the outer braided sleeve include the braid angle *q* [°], helical length L_{h} of one pitch of wire [mm], mandrel or braid diameter d_{b} [mm], wire width w_y [mm], and cover factor C [−].

One might argue that the pleated muscles are a kind of McKibben AMs using only parallel wires as the outer braided sleeve. These types of actuators outperform traditional McKibben AMs in terms of axial strain but exhibit drastically higher radial expansion due to the lack of radial-oriented wires in the sleeve. Due to the substantial differences between the pleated and biaxially braided McKibben AMs, we will not include these types of muscles in our review.

3.1.1. Braid angle

The ability of McKibben AMs to contract or extend depends on the initial braid angle θ [°] of the outer sheath, see figure 5. Both the axial strain and hysteretic behaviour of McKibben AMs are governed by the initial braid angle [39, 44, 45]. At the fully contracted position, the braid angle is set by the energetics of the operation of the AM at 54.7° [39]. The axial strain can be calculated using equations (3) and (8):

$$\varepsilon_{\max} = 1 - \frac{1}{\sqrt{3}\cos\theta} \tag{8}$$

Equation (9) assumes the actuator is under zero external load, with inextensible braid and fully

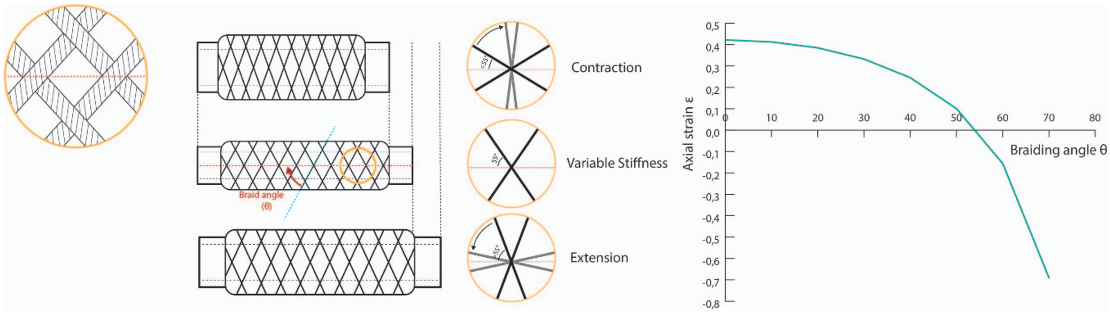

Figure 5. McKibben artificial muscle (AM) braid angle contribution to functionality. The braid angle is defined as the angle between the wires of the outer sleeve and the axial axis of the muscle. The braid angle determines the performance of the McKibben AM. Braid angles under 54.7° will result in contraction, braid angles at 54.7° will cause variable stiffness, and braid angles over 54.7° cause extension of the McKibben AM. The effect of the braid angle on the contraction ratio is schematically presented in the graph on the right-hand side.

pressurised [46]. From equation (9), the maximum theoretical axial strain can be determined when the contraction force nears zero [47]. From this, it is found that when θ is approximately 54.7°, the maximum axial strain becomes 0. Theoretically this means that McKibben AM with braiding angle of 54.7° generates no motion even if high pressure is applied, which makes them into a types of variable stiffness actuator. If the wires of the braid cross at an angle less than 54.7°, the radial expansion of the inner bladder will be transferred into axial compression and the McKibben AM will generate tension force at its ends. Braid angles over 54.7° result in axial extension.

The effect of the braid angle was experimentally investigated in a study by Gentry and Wereley [48]. They show that variations of the braid angle has a significant effect on the axial strain and the blocked force. It was found that contractile McKibben AM subjected to a pre-strained cyclic displacement test generated over 13 times the absolute blocking force and about 34% larger stroke than extensile AMs.

The minimum braid angle is limited by adjacent braid wires being forced against each other, assuming the inner bladder has a diameter small enough to allow for full braid dilation [39]. This minimum braid angle can, therefore, vary depending on the braid pattern, the wire material, and the diameter of the wire. Typically, the minimum braid angle is around 20° [6]. However, using a mathematical approach, Davis and Caldwell [39] showed that by halving the number of wires in the outer braided sleeve, the minimum braid angle can be reduced by 50% (from 19° to 9°) which results in an increase in the contractile range of the AM of approximately 7%, with a simultaneous peak contraction force increase of over 16% [39]. The minimum braid angle that can be obtained depends on the cover factor and can be calculated as follows [39],

$$\theta_{\min} = \frac{\sin^{-1}\left(\frac{2w_y m}{\pi D_0}\right)}{2}. \tag{9}$$

3.1.2. Wire elasticity

To prevent energy consumption during actuation, inextensible wires are preferred for the outer braided sleeve, such as high-stiffness aramid (Kevlar®) and ultra-high molecular weight polyethylene (Dyneema® and Spectra®) [49–51]. In the study of Krishnan *et al* [52] even silk is proposed as a braid material due to its higher stiffness than nylon and steel.

As can be observed in equation (1), the effect on wire elasticity on the contraction force and ratio is not considered. The inelastic braid assumption suggests that the outer braided sleeve of the McKibben AMs is inextensible to effectively convert the radial expansion of the bladder into axial contraction or extension of the muscle overall [53]. Although this assumption has often been cited as a likely source of model error, it keeps being used due to researchers' inability to directly measure the effects of braid elasticity [54]. However, a reduction in efficiency, both in terms of contraction force and axial strain, will be observed by the axial deformation of the wires. This is substantiated by the static model by Davis *et al* [29].

The effect of the wire stiffness, wire diameter, and wire structure on the blocking force was also investigated experimentally in a study by Hoque *et al* [36]. It was found that the stiffness of the wire was directly proportional to the AMs blocking force and axial strain. Furthermore, it was found that wire diameter governs the blocking force, with smaller wire dimension resulting in a reduced blocking force. Braided wires illustrated higher friction and, therefore, slightly lower free axial strains.

3.1.3. Cover ratio

The number and geometry of the wires that make up the outer braided sleeve can be expressed as the cover factor and is an essential property of a McKibben AM. The cover factor is defined as the ratio of area occupied by the wires within a periodic pore unit to the total area of the pore unit, as shown in figure 6. As derived by Sangian *et al* [55], the cover factor is

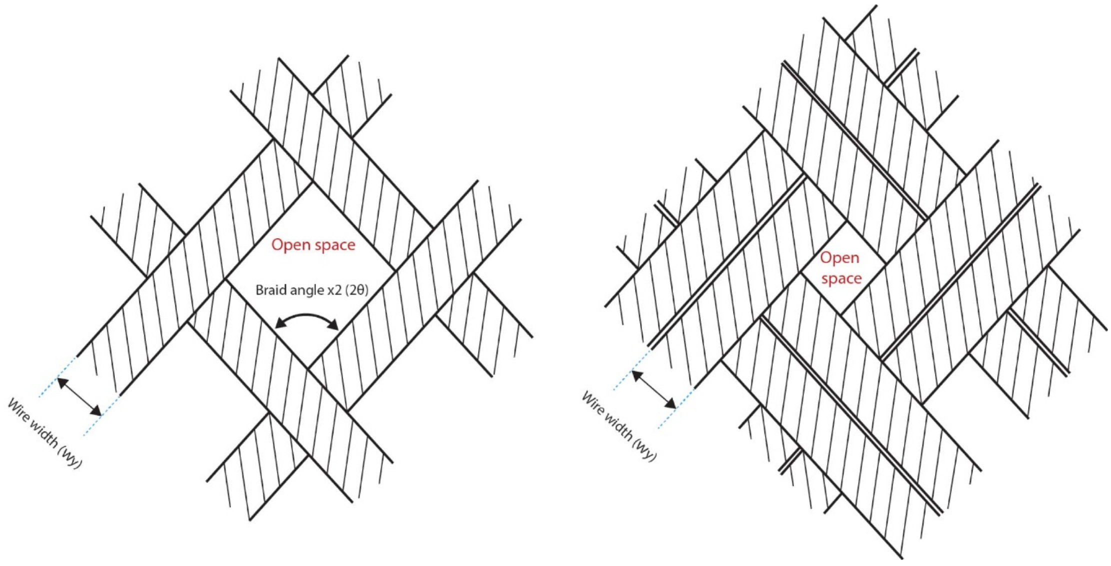

Figure 6. Outer braided sleeve cover factor of Mckibben artificial muscles (AMs). The cover factor is defined as the ratio of area occupied by the wires within a periodic pore unit to the total area of the pore unit. A cover factor of at least 0.7 for McKibben AMs is preferred to prevent bulging of the bladder through the outer braided sleeve. Using multiple wires or flat wires with increased wire width can be used to increase the cover factor (right),

described by equation (10) and is a function of the braid diameter D_0 [mm], the initial braid angle θ [°], the wire width w_y [mm], and the number of wires m [−].

$$C = \frac{w_y m}{\pi D_0 \cos\left(\frac{\theta}{2}\right)} - \left[\frac{w_y m}{2\pi D_0 \cos\left(\frac{\theta}{2}\right)}\right]^2 \tag{10}$$

Braided outer sleeves with high cover factors are normally required in manufacturing McKibben AMs due to the working conditions at high pressures. When fewer wires are used in manufacturing of the braided sleeve this results in wider gaps between the wires and consequently may result in rupture due to the internal bladder passing through the gaps at high pressures [1, 39]. In an effort to increase the cover factor, and thus the durability of the AM, on some occasions, multiple wires per direction or flat wires are used. Generally, a high cover factor of at least 0.7 is desired for proper functioning of the McKibben AMs, although examples of McKibben AMs exist with lower cover factors, such as 0.47 [1, 44].

3.2. Inner bladder configuration

An important geometrical property in determining the performance of a McKibben AM is the wire-to-bladder distance at the resting length. When the inner side of the braid structure is not in contact with the outer wall of the elastomeric bladder, the actuator's dead-band pressure increases dramatically since, when the bladder begins to expand, it is unable to transfer the force to the braiding structure and the actuator will remain inactive until the elastomeric bladder comes into contact with the braided sheath [53]. In equation (1), this distance is considered 0. Although friction decreases the efficiency of the muscles, as well as the contraction force, static friction between the wires themselves, as well the static friction between the inner bladder and wires, can increase the blocking force of the McKibben AM. Therefore, a trade-off remains.

By reducing the dead volume within the inner pneumatic bladder, the bandwidth of the McKibben AM can be increased by up to 400%, with a similar increase in stiffness [18]. To reduce the dead volume, different filler materials can be used, such as elastic particles, solid particles and liquids, with the added benefits of increased stiffness. At the same time, the air volume used to actuate the AM can be reduced by up to 80%–90% [18].

Strain energy losses could be reduced by preventing stretching of the inner pneumatic bladder, maximising the energy stored in the braids and the efficiency of the McKibben AM. In a study of Cavallaro *et al* [56], an oversized bladder containing radial folds was used. In the study by Meller *et al* [12], an inelastic LDPE bag was used as the inner bladder that unfolded during actuation. It was shown that this actuator had an efficiency of almost 80% and could achieve a blocking force of up to 500 N.

The Young's Modulus of the inner pneumatic bladder also plays an important role in determining the performance of McKibben AMs. In an experimental study by Hoque *et al* [36], it was found that a softer bladder, with a lower Young's Modulus, was able to generate higher free axial strains, with the risk of destructive failure. In addition, a larger diameter bladder was able to generate significantly higher blocking force but a lower axial strain on average due to the increased friction between the wires and the bladder [36]. In the study of Ball *et al* [57, 58], a model was presented that allows prediction of the effect of bladder pre- stretch, showing bladder pre-stretch results in higher actuator force and longer stroke length.

Modelling the inner pneumatic bladder is often challenging due to their complex non-linear deformations [59]. The literature on McKibben AM modelling mostly focuses on contractile AMs. However, Garbulinski *et al* [60] presents new hyper-elastic constitutive models and revalidate methods for extensile McKibben AMs that were previously studied for contractile McKibben AMs. The effect of hemi-spherical deformation of the inner pneumatic bladder near the end caps was investigated in the study by Kadowaki *et al* [61]. In their study, the inner pneumatic bladder was modelled as hemi-spherical, resulting in improved accuracy in the predication of the force-contraction profiles of McKibben AM.

4. McKibben muscle configurations

4.1. Natural Muscle types to McKibben configurations

McKibben muscles were originally designed to mimic natural muscles. Compared to natural muscles, McKibben AMs exhibit similar performance in terms of contraction strain at 20%–35%, as well as a higher tension intensity of 88–144 N cm^{-2} (versus 35 N cm^{-2}), higher work density of 0.13–0.20 J cm^{-3} (versus 0.13 J cm^{-3}), higher energy efficiency 0.32–0.49 (versus 0.2–0.25), and higher peak power density of 2.65 W cm^{-3} (versus 0.70 W cm^{-3}) [7, 62]. However, McKibben AMs lack the ability to be arranged as freely as natural muscles. McKibben AMs can approach the dynamic behaviour of skeletal muscles by carefully choosing an adequate outer braided sleeve [63]. To achieve the required force production, axial strain, and motion, for the intended application a specific type of muscle architecture might be required.

There are several muscle architectures that can be found in the natural world. Muscles are usually arranged in *parallel* or *pennate architectures*. In *parallel muscles*, the fascicles (motor-units of the muscles) run parallel to the axis of force generation. There are several parallel muscle architectures, such as *fusiform*, *convergent*, and *circular muscles*. A *convergent muscle* has a triangular or fan-shape as the fibres converge at its insertion and are fanned out broadly at the origin. A less common example of a parallel muscle is a *circular muscle* such as the *orbicularis oculi* in the eyelids, in which the muscle fibres are longitudinally arranged, but create a circle from origin to insertion. *Pennate muscles* differ from parallel muscles in that the fascicles attach obliquely (in a slanting position) to the tendon. This type of muscle generally allows higher force production but a smaller range of motion than *parallel muscles*.

4.2. Individual McKibben muscles

Individual McKibben Muscles take the shape of parallel natural muscles and can be found in a linear and circular configuration, see figure 7.

4.2.1. McKibben—linear

Bladder alterations: Whereas natural muscles can only contract to create moments and forces on their surroundings, McKibben AMs can also enable active extension depending on the braid angle. However, McKibben AMs differ from natural skeletal muscles in that they cannot perform passive elongation movements, in which the muscle is stretched by an external force from its natural length while deactivated. Since contractile McKibben AMs can only generate tensile force, they are often deployed in an antagonistic setup: two acting on opposite sides of a pulley, similar to the configuration of the triceps and biceps muscles controlling movement of the upper arm and elbow, respectively.

In studies by Tanaka *et al* [64] and Kobayashi *et al* [65], back-stretchable McKibben muscles are proposed that contract like a conventional McKibben AM when air pressure is applied and back-stretches like a natural skeletal muscle with no applied pressure (see figure 8). In the design by Tanaka *et al* [64], the inner bladder of the McKibben AM is extended and placed inside an inextensible flexible tube that is slightly bigger in diameter. In this set-up, when the muscle is not actuated, the inner bladder provides passive elongation when subjected to extension forces. However, whilst actuated, the inner bladder locks into position inside the inextensible flexible tube. In comparative experiments on a robotic arm, they achieved a 22% increase in the antagonist muscle driving range compared with conventional McKibben AMs without causing the muscles to sag significantly.

Another difference between McKibben AMs and their natural counterpart can be found in the way the sarcomere, the basic unit of a skeletal muscle, generates contraction. In the cross-bridge model of a sarcomere, the muscle accumulates nanoscale strokes of myosin head motors to generate larger strokes, similar to a ratchet-type mechanism, which makes the muscle more robust against mechanical disturbances and able to produce larger strokes. Taking inspiration from the nanoscale stroke method, the spring-like behaviour of McKibben AMs could potentially be negated, and large strokes could be generated that are independent from the applied load. Cho *et al* [66] developed a McKibben AM utilising two pawls integrated at both ends and a flexible rack inserted in the lumen, see figure 8. The ratchet-integrated McKibben AM was able to achieve a large stroke length of 250 mm (20 cycles) by accumulating

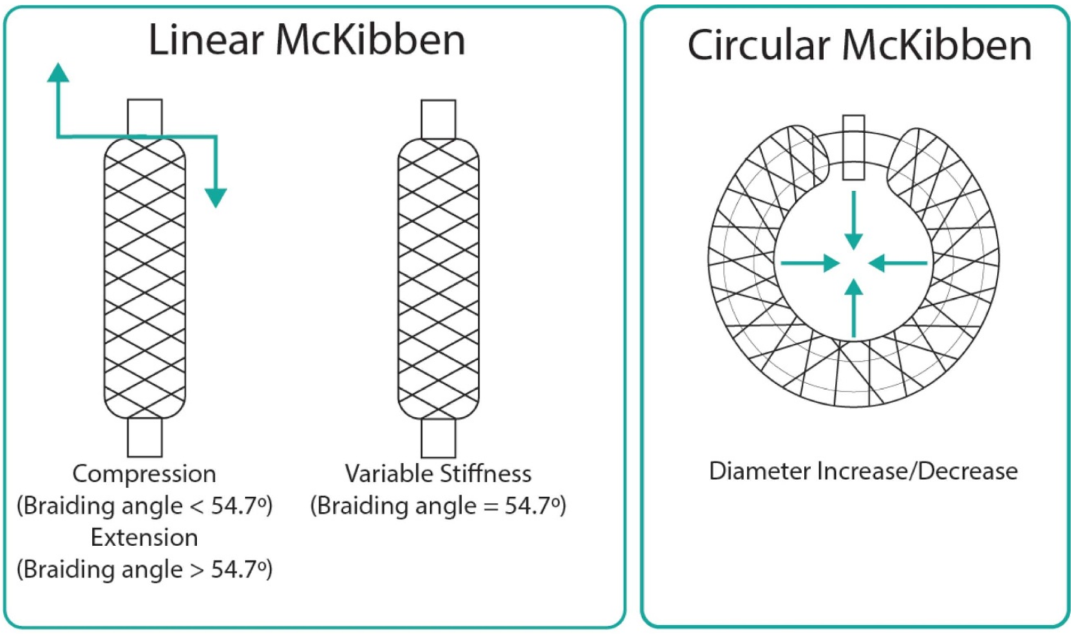

Figure 7. Individual McKibben artificial muscles (AMs) mimicking the functionality of parallel natural muscles. Linear McKibben AMs can either extend, contract, or illustrate variable stiffness during inflation. Circular McKibben AMs can be used to increase or decrease in diameter, similar to how a sphincter muscle operates.

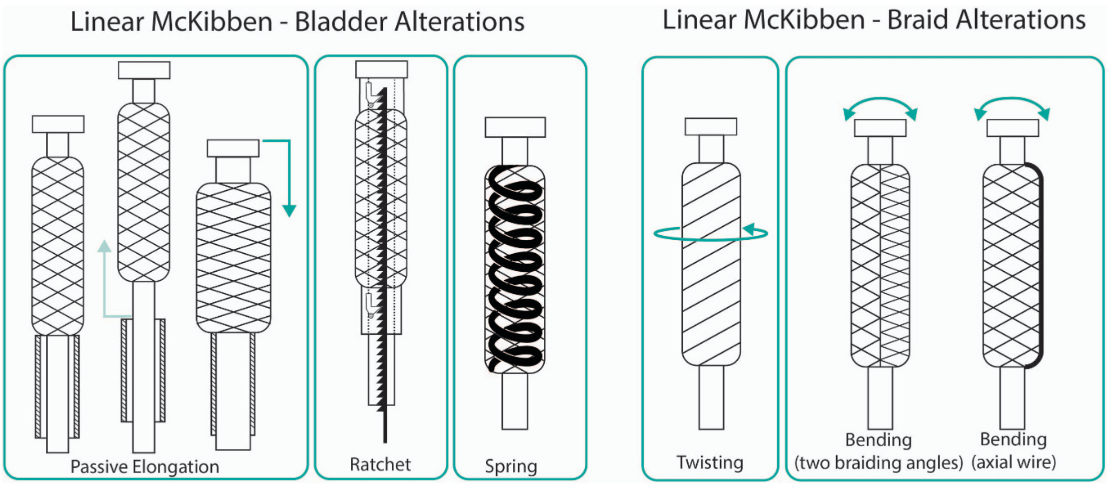

Figure 8. Linear McKibben artificial muscles Configurations found in Literature. Left: linear McKibben artificial muscles (AMs) with different bladder alterations. Passive elongation is seen in the back-stretchable McKibben developed by Tanaka *et al* [64], a ratchet mechanism is utilised in the McKibben AM developed by Cho *et al* [66], and a compression spring was added by Kim *et al* [67]. Right: Linear McKibben AMs with different braid alterations. A twisting McKibben AM was developed by Tian *et al* [68], a bendable McKibben AM using two distinct braiding angles was developed by Faudzi *et al* [69], and another bendable McKibben AM using an inextensible wire was developed by Feifei *et al* [70].

displacements from multiple small strokes by repeating the cycle of pressurisation and depressurisation. In comparison, a similar-sized regular McKibben AM was able to achieve a stroke length of approximately 30 mm. Cullinan *et al* [71] proposes a similar design that integrates a pulley system, resulting in a robust McKibben AM with simplified control [72].

Another bladder alteration is proposed by Kim *et al* [67], in which a low stiffness compression spring is added to the bladder to prevent buckling of the McKibben AM, see figure 8. By adding a compression spring to the McKibben AM, the effect of the axial strain on the contraction force is reduced, which makes this AM more suitable for use in large range of motion structures. Furthermore, a 31% greater contraction force and 26% higher contraction speed could be achieved in comparison to a conventional McKibben AMs, as well as a 21.5% increase in actuator efficiency. Finally, in a study by Legrand *et al* [73], a McKibben AM is proposed containing a working channel that can be used to guide other tools through during operation of the McKibben AM.

Braid Alterations: Next to extension and compression, individual linear McKibben AMs can also be used as variable stiffness actuators when the braid angle is set to 54.7°, resulting in an axial strain of 0. An example of such a variable stiffness McKibben AM is the one developed by Iwata *et al* [72].

Additionally, by removing one direction of the braid, the linear McKibben AM can be transformed into a twisting AM. In a study by Tian *et al* [68], a new fabrication process is proposed to realise twisting McKibben AMs by utilising braiding technology and water-soluble fibres, see figure 8. In the braiding process, half of the sleeve fibres of the AM is substituted with water-soluble fibres. Using this method, McKibben AMs with maximum twist angles of up to 160° could be obtained. Similarly, in the study of Olson and Menguc [74], a McKibben AM was helically wound around a compliant foam core to create a combined twisting and contraction motion with twist angles of up to 60°. In the study of Connolly *et al* [51] another twisting McKibben AM is illustrated.

Another braid alteration, in which two different braids are present on either side of the McKibben AM, can result in a bending motion. In the study by Faudzi *et al* [69], a McKibben AM (Ø 14 mm) was developed that contains two braids with different braiding angles (52 and 73°) on either side of the AM, which enable bending angles of up to 32°, see figure 8. The McKibben AM was manufactured by first embedding two separate braids into silicone, cutting these in half in the length direction, and finally attaching the two braided halves with a different braid angles to each other. In a follow-up study [75], the effect of the different weave pattern combination on the bending characteristics was researched using the Finite Element Method (FEM). It was found that the highest bending angles were obtained with braiding angle combinations of 32/90°, 32/70°, and 32/62° (in descending order of bending angle). Additionally, it was found that the braided layer needs to be placed close to the outer surface of the AM and the air chamber of the bladder needs to be large in order to increase bending performance [76].

Bendable McKibben AMs can also be obtained by partly restricting the movement of the braid in the axial direction. In the design proposed by Feifei *et al* [70], an inextensible wire is guided through the braid in the axial direction, which limits axial expansion of the McKibben AM at this side, see figure 8. Du *et al* [77] proposes a similar design in which an elastic support is connected to the braid to restrict unilateral axial displacement of the McKibben AM. It was show that bending angles of up to 90° were achieved in an experimental prototype. Finally, in the design by Xiang *et al* [78] a shape memory alloy wire was placed in parallel to an extending McKibben AM to initiate bending motions and in the study of Maeda *et al* [79] an shape memory polymer (SMP) was integrated into the braided sleeve of a McKibben AM to create bending and torsional motions.

4.2.2. McKibben—circular

No singular circular McKibben configurations have been identified

4.3. Bundled McKibben muscles

In figure 9, the potential parallel McKibben AM configurations are indicated.

4.3.1. McKibben—in series

By placing multiple contracting or extending McKibben AMs in series, the stroke can be increased, whilst maintaining the contraction force of a single McKibben AM. However, the system as a whole can only apply as much force as the weakest McKibben AM allows. Otherwise, the weakest AM would rupture or overstretch. The amount of contraction or extension of the full system (ΔL_{total}) is a summation of the individual stroke lengths (ΔL_k) pertaining to the McKibben AMs within the system, equation (11). The total axial strain is a length-weighted average of the axial strains of the individual AMs (ε_k), as shown in equation (12). This means that single McKibben AMs with longer initial length have more influence on the overall axial strain,

$$\Delta L_{\text{total}} = \sum \Delta L_k \tag{11}$$

$$\varepsilon_{\text{total}} = \frac{\sum \epsilon_k \cdot L_{0k}}{\sum L_{0k}}. \tag{12}$$

Placing an extensible McKibben AM in series with a contractile McKibben AM can initiate movement of a spacer that is placed in between the two AMs, as is seen in the study of Lathrop *et al* [80]. In this study, a contracting and extending McKibben AM were connected to each other via a cylindrical ring which was connected to a cable that actuated a steerable tip of a medical instrument.

Next to contraction or extension, a serial muscle arrangement can be used for creating locomotion motions, similar to the movement of an earthworm (figure 10). An example of this is given by the monoline drive design by Tsukagoshi *et al* [81]. In this McKibben AM (Ø 2.6 mm deflated, Ø 6.1 mm inflated), a travelling wave is generated using a single input pressure. For this purpose, the inner bladder of this McKibben AM contains a plurality of holes of different sizes to cause a time delay in chamber inflation and the outer braided sleeve is subdivided into multiple sections (chambers) using three tangential wires. This set-up makes it possible to induce a worm-like propulsion motion, as well as a bending motion, using a single input tube. The prototype was successfully tested in a lung model, illustrating its ability to successfully propel and steer through variable diameter branches. One might argue that this is a

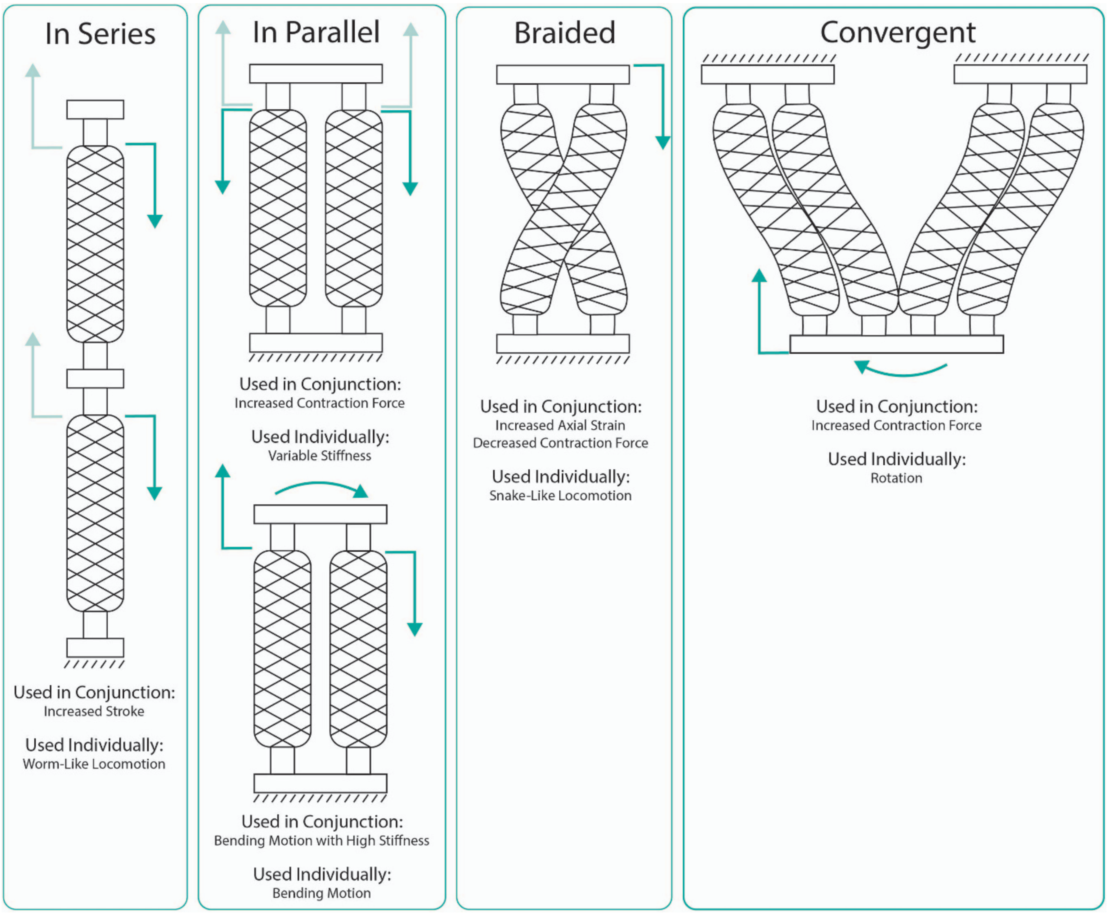

Figure 9. McKibben artificial muscle (AM) configurations mimicking the functionality of natural muscles. McKibben AMs can be placed in series, in parallel, can be braided or be placed in a convergent configuration. McKibben AMs placed in series can be used to increase the stroke or create worm-like locomotion. McKibben AMs placed in parallel can be used to increase the contraction force or to create bending motions (with high stiffness). Braided McKibben AMs have been shown to increase the contraction ratio, whilst simultaneously decreasing the contraction force. Furthermore, they can be used to create locomotion motions. Finally, convergent McKibben AMs can be used to increase the contraction force or create a rotation.

single McKibben AM, however, due to the use of different chambers, the McKibben AM functions as multiple AMs in series.

4.3.2. McKibben—in parallel

By placing McKibben muscles in parallel, the total contraction force of the McKibben AM can be increased without affecting the axial strain or stroke length. The total contraction force (F_{total}) is expressed mathematically as the summation ($\sum$) of individual contraction forces (F_{c}) pertaining to the McKibben AMs within the system:

$$F_{\text{total}} = \sum_{k} F_{\text{c}}. \tag{13}$$

Here, F_{c} signifies the contraction force of the kth McKibben AM. A similar strategy is seen in short parallel muscles, such as in the *biceps brachii*, located in the upper arm of the human body. The challenge with using multiple McKibben AMs in parallel is to attach the muscles in a space efficient way. In the study of Zhang *et al* [82], an improved multi-connector is proposed. Due to its detachable nature, the multi-connector can change contraction force and outer shape based on demand, meaning it can be applied to a wider range of fields.

In an experimental study of Kurumaya *et al* [38], it was shown that the axial strain of McKibben AMs can be increased by bundling, owing to its flexibility. The developed multifilament muscle comprised bundles of thin McKibben AMs and exhibited high deformability in comparison to conventional McKibben AMs of the same diameter. Furthermore, the interaction between the muscle fibres due to their radial expansion (similar to how a pleated AM functions), resulted in an 26% increase in the axial strain in comparison to a single McKibben AM. A design that takes advantage of this is illustrated by Bruder and Wood [83], in which two McKibben AMs are placed in parallel in a 'chain-link' actuator structure to achieve axial strains of over 50%.

A parallel McKibben AM muscle bundle can also function much like our skeletal muscle organs that selectively recruit a different number of motor fibres depending on the load demand [84]. A variable

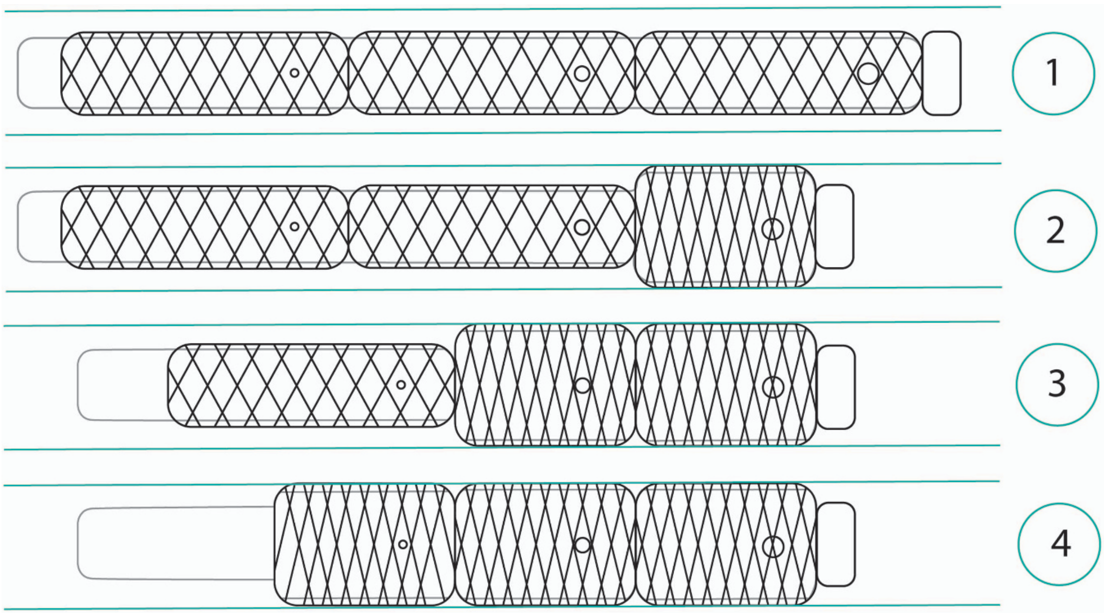

Figure 10. Mono-Line Drive McKibben artificial muscle (AM) Design by Tsukagoshi *et al* [81]. In the mono-line drive design, three McKibben AMs are placed in series. In the pneumatic inner bladder of the designs, three holes of different diameter are present that cause sequential inflation of the McKibben AMs. Step 1 indicates the resting position of the design. In Step 2, the distal McKibben AMs is inflated, causing it to anchor to the luminal wall. Step 3 and 4 indicates the sequential inflation of the middle and proximal McKibben AM.

recruitment McKibben AM bundle can adaptively activate the minimum number of AMs to increase its overall efficiency.

The parallel McKibben AM configuration can also be used to generate bending motions. Typically, McKibben AMs do not allow for bending motions, as in their natural state they either contract or extend and do not allow for passive extension. Therefore, in order to achieve bending motions, in general at least two McKibben AMs should be used in parallel for planar motions and three McKibben AMs for spatial motions, similar to how muscles attach to our bones to initiate the movement of our joints. In a study by Iwata *et al* [72], bendable and variable stiffness McKibben AMs were manufactured consisting of an extensible McKibben AM connected to a compressible McKibben AM. This way, both bending and variable stiffness could be achieved. Using two McKibben AMs with a diameter of Ø 21 mm, they were able to achieve a bending angle of 290°. Another bending configuration is proposed by Suzumori *et al* [85]. In this multi-filamented McKibben AM (Ø 21 mm), one central contracting McKibben AM and five surrounding extending McKibben AMs were bundled using non-elastic bands. Bending angles of up to 360° were reached in a 1.5 m long prototype. Similar bundled McKibben AM configurations are found in [86–91]. In the study of Lathrop *et al* [91], a slightly different approach was taken in which four contracting McKibben AMs were placed inside an outer slotted tube, that enabled bending motions of the structure.

Since McKibben AMs cannot passively lengthen, the performance of an antagonistic AMs configuration is decreased, similar what was previously described. In the study of Vocke III *et al* [92], the performance of an antagonistic McKibben AM system was increased by decreasing the passive parasitic force caused by the opposing AM. It was found that with the proper selection of design parameters, including mechanism geometry and McKibben geometry, an ideal McKibben AM configuration can be chosen that maximises deflection for a given arbitrary loading. In a study of Kang *et al* [17], flow dynamics of a pneumatic valve and thermodynamics of the inflating and deflating process are included to formulate the pressure variance of the antagonistic Mckibben AMs to yield better accuracy in high frequency motions.

4.3.3. McKibben—braided

Next to parallel arrangements, the McKibben AMs can be braided together to form one bigger braided AM. Braided McKibben AMs have been shown to increase the axial strain [93, 94]. In a study by Koizumi *et al* [93], it was substantiated that the axial strain of a biaxially braided McKibben AMs is larger than the axial strain of a single McKibben muscle. In this experimental study, the axial strain of braided McKibben AMs consisting of 8, 12, or 16 strands were compared with an individual McKibben AM and eight McKibben AMs placed in parallel, all with a length of 200 mm. The braided McKibben muscles showcased a contracting ratio of 0.37; a 9% increase compared to that of an individual McKibben AM. In addition, the contracting force per muscle was reduced by approximately 10% to 40% depending

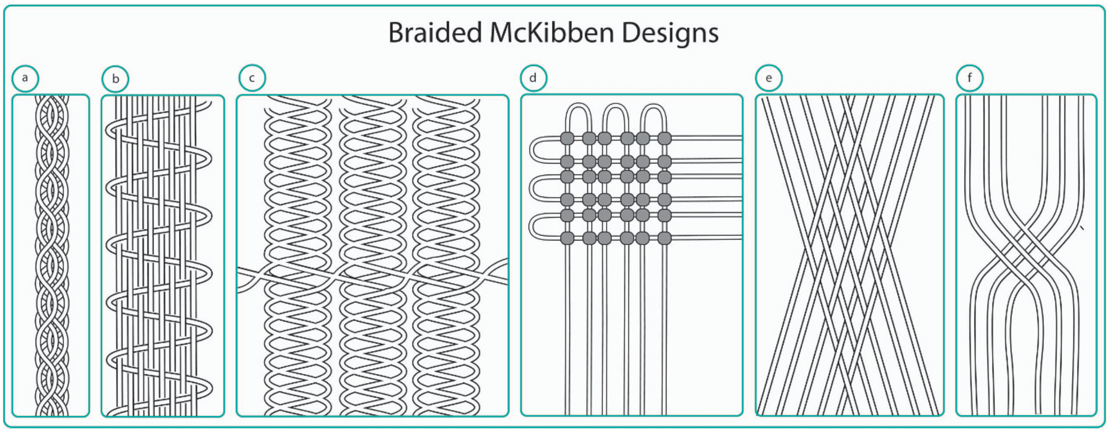

Figure 11. Braided McKibben artificial muscle (AM) Designs found in Literature. (a) Multi-braided structure, as proposed by Koizumi *et al* [93, 94], Kadir *et al* [95] and Na *et al* [96]. (b) Wefted McKibben AM structure, proposed by Abe *et al* [82], Hiramitsu *et al* [98] and Marshall *et al* [99]. (c) Interlaced braiding pattern in which one McKibben AM is interchanged between the braids at certain instances, as proposed by Kurumaya *et al* [49]. (d) McKibben AM configured in a grid-like pattern with thin plastic plates between layers, square clamps at intersections, and each McKibben AM folded back on itself to double the output force, as proposed by Funabora *et al* [100]. (e) Cross-shaped braiding pattern, as proposed by Funabora *et al* [5, 101]. (f) Cross-shaped braiding pattern of an active textile developed by Nakagawa *et al* [102].

on the braiding angle, due to the increase in friction between the muscles. A similar result was observed in the study of Kadir *et al* [95], in which the axial strain significantly increased in a braided architecture, at the cost of the contraction force.

In a follow-up study, Koizumi *et al* [94] developed a double-braided structure increasing the axial strain even further towards 0.41. It was found that there is a positive correlation between the number of braid cycles and the maximum axial strain, which allowed for achieving axial strains of up to 0.41 with a double-braided muscle, versus 0.36 in a single-braided muscle. However, the axial strain was approximately 11% lower than what was found in the analytical model, which is hypothesised due to the increase of friction as the number of braiding cycles increases, which in turn is due to the increase in the number of contact points between the muscles [94].

Another major advantage of using a braided structure is its ability to be elongated by applying an external force. Current parallel McKibben AMs cannot passively or actively extend like natural muscles, which make their use in antagonistic set-ups challenging, as previously discussed. In the study of Na *et al* [96], they investigated the ability of the double-braided structure proposed by Koizumi *et al* [94] to be actively stretched for use in an antagonistic set-up. They demonstrated that the driving range of joint angle actuated by braided McKibben AMs (joint angle of 73°) was larger than that of the unbraided McKibben AMs (joint angle of 88°).

A different braid pattern was proposed by Abe *et al* [97]. In this study, the '18 Weave' pattern is proposed in which one McKibben AMs is guided through wefted McKibben AMs, see figure 11. Whilst the axial strain is significantly lower than the braided structure developed by Koizumi *et al* [94], an advantage of this structure is its flat configuration, which is advantageous in, for example, exosuits or garments. Kurumaya *et al* [49] developed yet another flat and flexible braided McKibben structure consisting of three braided strands that are interlaced by exchanging a single muscle strand with each other at specific positions along the length of the muscle. This braided structure showed exceptional flexibility in comparison to the ones developed by Abe and Koizumi *et al* [93, 94, 97]. The experimental results demonstrated that the initial braiding pitch influences both the contraction force and the axial strain. A maximum contraction force of 14.8 N and maximum axial strain of 0.34 was found using these braided muscles [49].

By integrating McKibben AMs into external structures or matrices through weaving or braiding, a wider range of movement patterns, such as twisting and bending motions, can be achieved. In a study conducted by Funabora *et al* [100], 18 McKibben AMs were arranged in a 5 × 4 grid structure with thin plastic plates between layers, square clamps at intersections, and each muscle folded back on itself to double the output force. This setup was integrated into a garment to induce bending and twisting motions of the back of the user. Subsequently, Funabora [101] developed an active textile where 12 McKibben AMs were woven through a flexible rubber structure in a cross-shaped pattern to enable in-plane and out-of-plane bending, as well as twisting motions. Similar cross-shaped pathways are observed in an active textile developed by Nakagawa *et al* [102], where 28 McKibben AMs were embroidered onto a flexible textile, enabling in- and out-of-plane bending, as well as twisting motions, similar to the design by Funabora [101].

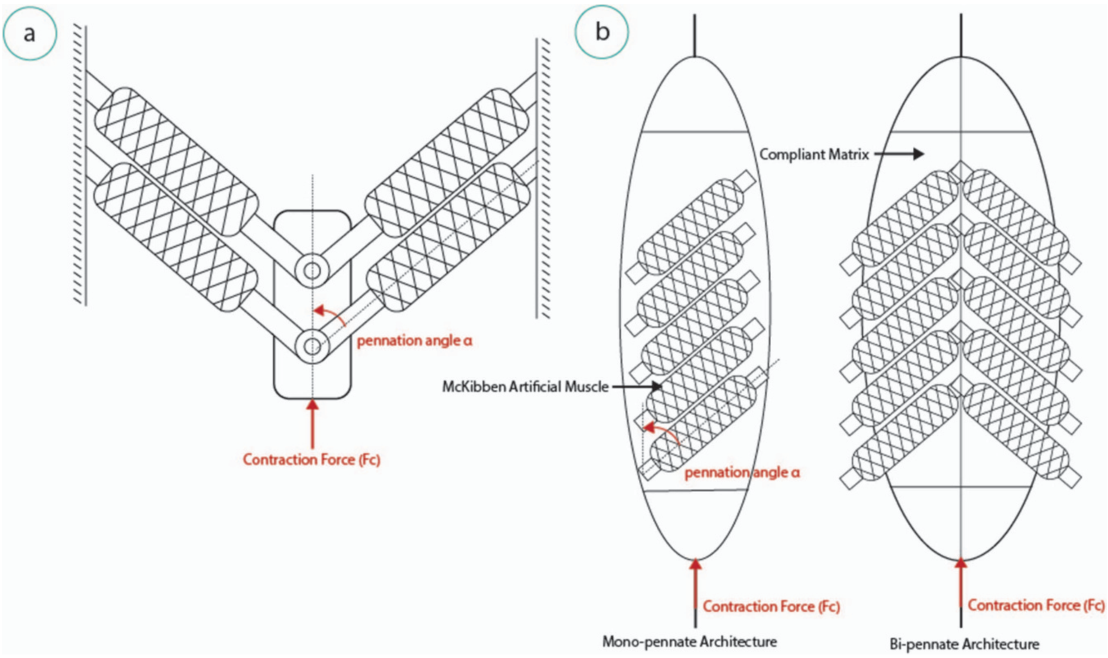

Figure 12. Pennate McKibben Artificial Muscle Designs found in Literature: (a) Bi-pennate muscle architecture proposed by Duan *et al* [103] and Azizi *et al* [104] and (b) Pennate and bi-pennate architecture embedded in a compliant matrix proposed by Wang *et al* [105].

In the research conducted by Hiramitsu *et al* [98], McKibben AM were integrated into textile structures, comprising fabric strings or strips arranged in a plain weave pattern. Within this pattern, one McKibben AM was intricately woven through the structure, serving as the thin warps, while the wefts consisted of strings or strips constituting the textile. Through this configuration, a contractile active textile was realised. A similar architectural approach was observed in the study conducted by Marshall *et al* [99]. Their findings revealed that lower muscle density corresponded to increased thickness during expansion and reduced axial strain of the active textile.

A further iteration was made by Hiramitsu *et al* [106], in which active textiles were proposed that can achieve bending motions. In addition to a plain weave, in this study a twill weave and sateen weave pattern, in which a different amount of McKibben AM run on the front and back of the textile, were used to initiate bending motions. It was found that the characteristics of the wefts (AMs that run horizontally) and warps (AMs that run in vertically), such as cross-sectional shape, bending stiffness and elasticity, determine the characteristic of the active textile.

4.3.4. McKibben—convergent

Multifilament muscles can have various shapes and can mimic the shape of human muscles, including convergent configurations [38]. The advantages of multifilament muscles are that the points of force application are easily altered and the output force increases in proportion to the number of bundled muscles [38]. A convergent muscle configuration was found in the study of Kurumaya *et al* [107]. In this study, two different types of convergent muscle configurations were developed: (1) using two bundles of 60 McKibben AMs divided by an angle of 30° similar to the biceps muscle and (2) using 16 McKibben AMs that fan out, resulting in a flat muscle similar to the deltoid muscle. A axial strain of approximately 0.2 was found for each set-up.

4.3.5. McKibben—pennate

Studies focusing on McKibben AMs often focus solely on the contractile elements and rarely address the contribution of flexible connective tissue that forms an integral part of the morphology of biological muscle. A fundamental feature of pennate muscles is that muscle fibres are oriented at an angle to the line of action and rotate as they shorten, becoming more oblique throughout a contraction (figure 12). This change in fibre orientation (pennation angle) can amplify the shortening velocity of a fibre and increase output velocity, output force and work output capacity of the muscle [103, 104].

The velocity advantage resulting from dynamic changes in the pennation angle can be characterised as a gear ratio or amplification factor (muscle velocity/fibre velocity). A pennate muscle's gear ratio varies automatically depending on the load such that a muscle operates with a high amplification during rapid contractions and low amplification during forceful contractions. Muscle force is attenuated by the cosine of the pennation angle and a change in fibre displacement is amplified by the secant of the pennation angle [108]. For a contractile pennate actuator at a constant pressure, the initial configuration represents the maximum force because it is the minimum pennation angle [108]. The transmission ratio TR_{force} of the input to the output force can be found using the following equation [108]:

$$TR_{force} = \frac{F_m}{xF_c} = \cos\alpha. \quad (15)$$

With F_m the muscle force exerted by the pennate architecture set-up, x the number of individual McKibben AMs in the set-up, F_c the contraction force per muscle in line with the axial axis of each individual McKibben AM in the set-up, and a the pennation angle, which is defined as the angle between the McKibben AMs and the vertical attachment point.

The muscle force F_m of a bipennate architecture can be calculated using the following equations:

$$F_m = \cos\alpha x F_c. \quad (16)$$

Azizi *et al* [104] showed that a pennate-like McKibben AM array can mimic the variable gearing mechanism of natural pennate muscles. When the array contracts against light loads, the individual McKibben AMs undergo changes in pennation angle, the array increases in thickness and produces a large displacement. Conversely, when the array contracts against heavy loads, the individual McKibben AMs rotate less, the array increases less in thickness, produces a smaller amount of displacement and a higher contraction force. As a result, the actuator is automatically adapted to the specific task.

In the study by Wang *et al* [105], McKibben-type AMs were integrated into a flexible matrix in a pennate architecture. The developed actuators demonstrate that the material properties of both the contractile units and connective tissue play a crucial role in force generation, force transmission and deformation.

5. New avenues: smart McKibben muscles

5.1. Smart braided sleeves and inner bladders

The braided outer sleeves of McKibben AMs are crucial for their performance. The main function of the braided sleeve is to convert the radial expansion of the inner bladder to axial compression or extension. However, the outer braided sleeve could be used to alter the performance of the McKibben AM or add extra functionalities, including sensing capabilities [75, 109–123]. The braided sleeve of the McKibben AMs could be sensorised by using smart wire materials.

Conductive wires are able to sense contraction and force by measuring the changes in coil inductance [109, 110, 112, 114, 116, 117, 120, 124]. In a study by Wakimoto *et al* [120], a McKibben AM with an internal pressure-sensing function was proposed by using one conductive wire in the sleeve. The applied pressure on the McKibben AM was estimated by observing the electrical resistance of the conductive fibre. Furthermore, research by Felt and Remy [125] has shown that measuring the axial strain and force is possible by interlacing conductive, insulated wires through the braided sleeve. These wires act as a solenoid-like circuit with an inductance that more than doubles when the McKibben AM contracts. A similar design was proposed by Erin *et al* [109]. In this study, an inductive coil was wrapped around the outer braided sleeve, which allowed for measuring the contraction force and the displacement through the changes in coil inductance.

Conductive materials and mechanisms can also be added to the McKibben AM to enable displacement sensing. Wakimoto *et al* [121, 126] proposed a sensor made out of rubber and a conductive film integrated into the inner pneumatic bladder. The dielectric elastomer sensor designed by Kanno *et al* [113] consisted of thin, highly compliant dielectric and conductive membranes, which allowed the length of the actuator to be detected by reading the capacitance. The sensor directly wrapped around the inner tube of the McKibben AM. Other studies proposed conductive rings placed concentric to the outer braided sleeve of the McKibben AM to enable radial expansion sensing. Zhong *et al* [123] proposed a soft radial sensor placed around the McKibben AM composed of liquid metal (gallium-indium-stannum) and a silicone substrate, whereas Kuriyama *et al* [127] proposed an electro-conductive rubber ring. Additionally, piezo-resistive sensor placed in parallel to the McKibben AM [115], a flexible strain sensor [111], a nylon string coated sensor attached to the braid [128], and a telescopic capacitive length transducer inside the lumen [129], were proposed.

Optical fibres for contraction and shape sensing were proposed by [118, 119, 122]. In the studies of Tian *et al* [118] and Yoshimoto *et al* [122] a step-index multimode optical fibre was integrated in the McKibben AM, and the length was estimated based on the change in the amount of light propagating in the optical fibre. Akagi *et al* [130] proposed another optical method to measure displacement in which a photoflector was placed in the inner lumen of the McKibben AM to measure the distance to the inner pneumatic bladder during inflation.

Other designs incorporate a piezo-resistive sensor placed in parallel to the McKibben AM [115], a soft radial sensor placed around the McKibben AM composed of liquid metal (gallium-indium-stannum) and a silicone substrate [123], a dielectric elastomer sensor integrated into the inner pneumatic bladder [113, 131], a flexible strain sensor [111], a nylon string coated sensor attached to the braid [128], a photoflector placed in the inner lumen [130], a telescopic capacitive length transducer inside the lumen [129], and an electroconductive rubber ring placed concentric to the actuator [127]. The dielectric elastomer sensor designed by Kanno *et al* [113] consisted of thin, highly compliant dielectric and conductive membranes, which allow the length of the actuator to be detected by reading the capacitance. In the study of Kumar *et al* [37], a hybrid McKibben AM was proposed containing a dielectric bladder. A mathematical model for this type of actuator is given by Goulbourne [132].

In a study by Yahara *et al* [133], a smart outer sleeve was developed containing helical SMP fibres. The SMP wires allowed for changing the braiding angle after fabrication, which in turn allowed for active alteration of the performance of the McKibben AM. In the study by Takashima *et al* [134], the outer sleeve of a commercially available McKibben AM was impregnated with SMP resin. By actuating this McKibben AM over the glass temperature (T_g), it functions as a regular McKibben AM. However, the McKibben AM can be cooled down below T_g to fix the AM in this rigid, actuated, state. Smart materials were also used in the study of Lopez-Diaz *et al* [135], in which a self-healing hydrogel polymer was used as the inner pneumatic bladder of the McKibben AM. The developed self-healing hydrogel was able to self-heal without the need for an external stimulus, which could be beneficial to improve the durability of the AM in the future.

5.2. Alternative manufacturing methods

Current McKibben AMs are mainly manufactured using lab-scale braiding machines [1]. Although these machines offer high precision, they suffer from several essential disadvantages. Firstly, the braiding machines are limited in generating only a narrow range of braid angles. Secondly, producing a consistent cover factor is limited due to the friction between fibres. Third, long fibre lengths are needed to operate braiding machines, which limit the introduction of novel fibre materials for research-scale production especially when only short lengths of experimental fibres are available [1].

An alternative way to manufacture braided sleeves is by using additive manufacturing or 3D-printing [1]. 3D-printing allows for improved versatility in controlling the materials, geometry and the structure of the braids, as well as allow for direct printing of the end connectors of the AM. In a study by Sangian *et al* [136], an extrusion style 3D-printing machine was used to manufacture a smart braided sleeve with a cover factor of 0.47. Each individual printed wire was made of PolyCaproLactone (PCL) and was precisely printed around a rotating cylindrical steel rod. The right to left printing direction was first performed and then the entire mandrel with the printed helix was dip-coated in alginate solution and dried. Subsequently, the left to right printing direction was performed to form the second helical fibre on top of the dry alginate film. The mandrel was then immersed in the water bath to dissolve the alginate interlayer.

5.3. Alternative braided sleeves

The majority of the McKibben AMs use a biaxial braiding pattern. Alternative braiding patterns are rarely explored. Furthermore, other braiding methods, including triaxial braids could be explored. In triaxial-braided fabric three sets of wires are used and intertwined with each other around straight wires at about a 45° angle. In this method, braiding very dense structure patterns is less feasible compared to biaxial-braided fabrics, but the axial directional properties are improved in this method. A major downside of this braiding method is the presence of the axial braiding wires, which will counteract the compression or extension in the muscle. Therefore, if this type of braiding technique is considered, either elastic or free-moving axial wires should be used. A knitted McKibben AM was developed by Ball *et al* [137] in which the sleeve expands by letting the loops of fibre slide past each other, changing the dimensions of the rectangular cells in the stitch pattern. Preliminary tests showed that free contraction greater than 50% is achievable using this knitting pattern. However, the motion relied on using fibres with low coefficient of friction in order to reduce hysteresis.

In a study by Bennington *et al* [138], a viscoelastic sheath was added to the outer sleeve. It was shown that different polymeric sheaths could augment the shape of a standard McKibben AM's force-velocity curve. Another alternative outer sleeve was presented by Naclerio *et al* [139] in which a thin, single layer of woven, bias-cut fabric was used that was foldable when depressurised. The airtight fabric was adhered together with a flexible adhesive, negating the need for an inner bladder. Experiments showed less than 1% hysteresis. Similarly, a bellows-shaped outer sleeve was proposed by Risangtuni *et al* [140] achieving an elongation ratio of almost 70%.

5.4. Alternative actuation methods

A major failure mode of McKibben AMs is rupture of the inner pneumatic bladder. In an effort to overcome this, research has been conducted to manufacture bladderless McKibben AMs. A bladderless McKibben muscles was developed by Sangian *et al* [55], in which a thermally expanding paraffin wax was used to replace the bladder. This paraffin wax was contained within an electrically conductive braid which allowed for Joule heating of the paraffin. Using this method, Sangian *et al* [55] was able to manufacture a lightweight muscle of 0.14 g with a diameter of 1.4 mm which was capable of generating a tensile stress of 50 kPa (0.039 N) in 20 s. The maximum axial strain of 0.1 was achieved in 60 s. In the study by Salahuddin *et al* [141], a hydrogel-filled McKibben AM was proposed. In this design, the inner pneumatic bladder was replaced by thermo-responsive hydrogel beads that can swell in the presence of water. The hydrogel McKibben AMs were able to achieve a blocking force of 5–6 N and an axial strain of 0.07–0.08, although the response time was very low (>1 h).

One of the challenges for McKibben AMs is that they generally need air hoses and air sources like compressors for actuation, which can lead to bulky systems overall. Chemo-mechanical transformations can be used to produce a mechanical force from a reversible chemical reaction to generate muscle contraction. Nabae *et al* [142] propose an electrically driven McKibben AM (Ø 4 mm) using a tube-shaped polymer electrolyte fuel cell (PEFC) using platinum electrodes. In this design, the tube-shaped PEFC was used to initiate a reversible gas/liquid chemical reaction inside the McKibben AM to initiate expansion, generating an axial strain of 0.047. In a follow-up study by Kodaira *et al* [143], the axial strain (0.22), response time (35 s) and durability of the PEFC was improved by using an Au/Pt double-layer electrode which decreased the appearance of cracks in the electrode. In the study of Vial *et al* [144], another chemo-mechanical reaction was proposed to actuate a McKibben AM (Ø 15 mm) in which a granular ion-exchange polymer was placed inside the inner pneumatic bladder. The addition of acidic (NaOH) or alkaline (HCl) solutions provoked a swelling-deswelling cycle, respectively, resulting in an axial strain of 0.2, a blocking force of 332 N, and a response time of 1313s. A similar approach was proposed by Tondu *et al* [45].

Creating fully untethered McKibben AMs involves integrating self-contained pneumatic or other actuation system within the muscle structure to provide on-board actuation, eliminating the need for external tethers. An untethered McKibben AMs was proposed by Mirvakili *et al* [145], in which a magnetically induced liquid-to-gas phase transition of a liquid created a volumetric expansion (steam) and thus developed sufficient pressure inside the McKibben AM for mechanical operations. The untethered McKibben AM was able to generate actuation strains of up to 20% (in 10 s). A stretchable electrically-driven driven pump for McKibben AMs was proposed by Cacucciolo *et al* [146]. This pump was able to directly accelerate liquid molecules by means of an electric field, requiring no moving parts, obtaining a blocking force of 0.84 N and a maximum axial strain of 0.02. In the paper by Sangian *et al* [46], a small-size, fully enclosed, hydraulic McKibben muscle powered by a low voltage pump connected to a 25 ml water tank was investigated. These muscles were able to generate a blocking force up to 26 N and strains up to 23% at a water pressure of 2.5 bar.

6. Discussion & conclusions

6.1. Summary of main findings

This review paper summarises the latest advancements in the development of McKibben AMs, highlighting their performance and unique configurations. Innovations in McKibben AM design have led to enhanced performance characteristics, including increased force output, improved efficiency, and greater durability. By mimicking natural muscle configurations, intricate motions can be created, including bending motions, linear motions and twisting motions. Smartly placing McKibben AMs in flexible or soft structures can lead to intricate motions overall. Different architectures provide distinct performance advantages. Series configurations increase overall stroke and enable worm like or peristaltic locomotion. Parallel configurations enhance force output and can provide variable stiffness, bending, twisting, or antagonistic behaviour. Braided configurations can increase achievable strain and facilitate flat or textile integrated actuator geometries. Convergent assemblies improve force density by combining multiple actuators into a shared output node, while pennate configurations offer a tunable trade-off between force and shortening velocity by adjusting the pennation angle.

Current McKibben actuators still exhibit several inherent limitations. Efficiency remains constrained by elastomer viscoelastic losses [12]. Hysteresis and friction, originating from bladder viscoelasticity, braid elasticity and strand on strand interactions, impede precision [39, 53, 54]. Environmental sensitivity also remains significant as material durability is affected by temperature fluctuations and humidity [147]. In addition, scaling effects become dominant as actuators shrink, altering pressure–flow relationships and mechanical response [14].

Recent developments offer promising avenues to mitigate some of these limitations. Additive manufacturing and textile based architectures improve customisation and achievable strain. For example, 3D printed braided sleeves enable precise control over braid angle and cover factor, offering more versatile geometry tuning than traditional McKibben AMs [1, 136]. Similarly, knitted sleeves [137] and multifilament braided designs [93, 97] enable flat or textile integrated actuators, and can increase attainable contraction stroke. However, these approaches still face material fatigue and hysteresis constraints inherited from elastomeric bladders and fibre friction [93, 97, 137].

Smart material based approaches further expand design possibilities. SMP braids can tune contraction characteristics [133] and stiffness [134] during operation, while self-healing hydrogel based McKibben actuators provide autonomous damage mitigation that may improve durability [135]. In parallel, bladder free or non-fluidic McKibben type actuators eliminate the need for compressors or pumps and avoid leakage, trading untethered integration for slow response times or thermal constraints [55, 141, 145]. Overall, these material innovations address long standing challenges such as fatigue resistance, leakage, and system integration, but hysteresis and bandwidth limitations remain challenges that these new designs alone do not fully overcome.

Although the present review focuses on the design and performance characteristics of McKibben AMs, it is important to acknowledge the main application domains that have shaped their development. Broadly, McKibben AMs are often employed in wearables and prosthetics, where they assist or restore human motion through exoskeletons, orthotic devices, prostheses, and rehabilitation systems. Depending on the required wearability and compliance, they are either mounted on rigid frames or integrated into garments or soft matrix structures. A second major domain is robotics and manipulation, including humanoid platforms, soft and continuum manipulators, and a variety of locomotion systems. These application areas highlight the versatility of McKibben actuators and proves the importance of understanding design parameters in the context of practical deployment.

6.2. Limitation of this study

One limitation of this study arises from the exclusive focus on papers that specifically include the word 'McKibben' in their title or abstract. This approach inherently restricts the breadth of the literature reviewed, potentially overlooking relevant studies that examine McKibben AMs under alternative terminologies or broader categories of pneumatic AMs. Our scope is limited to actuators explicitly described as McKibben muscles with external braided sleeves. We acknowledge that this excludes certain fibre-reinforced elastomer actuators and McKibben-like designs. Consequently, important insights, comparative analyses, and advancements documented in research that uses different nomenclature or focuses on similar AM technologies may be excluded, leading to a narrower understanding of the current state of knowledge and development in the field. For example, fibre-reinforced elastomeric enclosures fall outside our formal search results due to terminology differences, but their related studies present interesting architecture-level design strategies using nested series configurations to amplify stroke [148] and pennate arrangements to trade force and contraction [149]. Future reviews could benefit from a more inclusive search strategy that encompasses a wider array of related terms and research contexts to capture a more comprehensive picture of the advancements and challenges associated with McKibben AMs. Additionally, for comparison of performance characteristic of different muscle like actuators (e.g. electroactive polymers, shape-memory alloys, carbon-nanotube actuators, and other fluidic AMs), we would like to refer the reader to existing comprehensive reviews [150].

6.3. Recommendations for future research

Future research on McKibben AMs should prioritise several critical areas to enhance their performance and expand their applicability. Innovations in material science are essential, focusing on developing new composites and elastomers that improve durability, flexibility, and responsiveness of the inner pneumatic bladder, thereby addressing issues like fatigue resistance and operational lifespan. Efforts to improve energy efficiency will make McKibben AMs more viable for portable and long-duration uses, potentially involving optimised pneumatic systems or alternative actuation methods. Miniaturisation of these actuators is another key area, particularly for expanding their use in medical devices such as minimally invasive surgical tools and wearable technologies, which requires maintaining strength and efficiency at smaller scales. Existing studies indicate that miniaturisation can significantly alter pressure–force behaviour and maximum stroke, but a unified scaling framework is still lacking [14]. We therefore highlight the development of such scaling laws as an important direction for future research. Finally, developing application-specific designs tailored to the unique demands of different fields can maximise the effectiveness and versatility of McKibben AMs.

Data availability statement

All data that support the findings of this study are included within the article (and any supplementary files).

ORCID iDs

V G Kortman 0000-0002-2370-0013
J Jovanova 0000-0001-8347-6386
H Nabae 0000-0002-3036-6447
A Sakes 0000-0002-4323-884X

References

[1] Sangian D 2021 From traditional braiding methods to additive manufacturing for fabricating Mckibben artificial muscles *Biomed. J. Sci. Tech. Res.* **38** 30728–35
[2] De Volder M, Moers A J M and Reynaerts D 2011 Fabrication and control of miniature McKibben actuators *Sens. Actuators A* **166** 111–6
[3] Mori M, Suzumori K, Takahashi M and Hosoya T 2010 Very high force hydraulic McKibben artificial muscle with a p-phenylene-2, 6-benzobisoxazole cord sleeve *Adv. Robot.* **24** 233–54
[4] Schulte H 1961 The characteristics of the McKibben artificial muscle *The Application of External Power in Prosthetics and Orthotics* (National Academy of Sciences) pp 94–115

[5] Tondu B and Lopez P 2000 Modeling and control of McKibben artificial muscle robot actuators *IEEE Control. Syst.* **20** 15–38
[6] Caldwell D G, Medrano-Cerda G A and Goodwin M 1995 Control of pneumatic muscle actuators *IEEE Control Syst.* **15** 40–48
[7] Chou C-P and Hannaford B 1996 Measurement and modeling of McKibben pneumatic artificial muscles *IEEE Trans. Robot. Autom.* **12** 90–102
[8] Thomalla S D and Van De Ven J D 2018 Modeling and implementation of the McKibben actuator in hydraulic systems *IEEE Trans. Robot.* **34** 1593–602
[9] Iwata K, Suzumori K and Wakimoto S 2012 A method of designing and fabricating McKibben muscles driven by 7 MPa hydraulics *Int. J. Autom. Tech.* **6** 482–7
[10] Yokota S and Komatsu T 1994 Flexible hydraulic actuator for space manipulators *JSME Int. J. Ser. C* **37** 179–84
[11] Zhang Z, Hou J, Ning D, Gong X and Gong Y 2017 Modeling and experiments on the drive characteristics of high-strength water hydraulic artificial muscles *Smart Mater. Struct.* **26** 055023
[12] Meller M A, Bryant M and Garcia E 2014 Reconsidering the McKibben muscle: energetics, operating fluid, and bladder material *J. Intell. Mater. Syst. Struct.* **25** 2276–93
[13] Solano B and Rotinat-Libersa C 2011 Compact and lightweight hydraulic actuation system for high performance millimeter scale robotic applications: modeling and experiments *J. Intell. Mater. Syst. Struct.* **22** 1479–87
[14] Peel L D, Muratalla L, Baur J and Foster D 2011 The effect of scale on fluid-filled flexible composite actuators *ASME 2011 Conf. on Smart Materials, Adaptive Structures and Intelligent Systems, SMASIS 2011* vol 2 pp 581–90
[15] Kobayashi W and Ito K 2015 Displacement estimation of tap-water driven McKibben muscles *Proc. 2015 Int. Conf. on Fluid Power and Mechatronics, FPM 2015* pp 672–6
[16] Olson G, Manjarrez H, Adams J A and Menguc Y 2022 Experimentally identified models of McKibben soft actuators as primary movers and passive structures *J. Mech. Robot.* **14** 011006
[17] Kang B S, Kothera C S, Woods B K S and Wereley N M 2009 Dynamic modeling of McKibben pneumatic artificial muscles for antagonistic actuation *Proc. IEEE Int. Conf. on Robotics and Automation* pp 182–7
[18] Davis S, Canderle J, Artrit P, Tsagarakis N and Caldwell D G 2002 Enhanced dynamic performance in pneumatic muscle actuators *Proc. IEEE Int. Conf. on Robotics and Automation* vol 3 pp 2836–41
[19] Wenlin C *et al* 2021 Experimental study on dynamic characteristics and fatigue of McKibben pneumatic artificial muscles *2021 IEEE Int. Conf. on Real-Time Computing and Robotics, RCAR 2021* pp 223–6
[20] Al-Ibadi A, Nefti-Meziani S and Davis S 2016 Valuable experimental model of contraction pneumatic muscle actuator *2016 21st Int. Conf. on Methods and Models in Automation and Robotics, MMAR 2016* pp 744–9
[21] Belforte G, Raparelli T and Sirolli S A 2017 A novel geometric formula for predicting contractile force in McKibben pneumatic muscles *Int. J. Autom. Tech.* **11** 368–77
[22] Hocking E G and Wereley N M 2012 Analysis of nonlinear elastic behavior in miniature pneumatic artificial muscles *Smart Mater. Struct.* **22** 014016
[23] Kothera C S, Jangid M, Sirohi J and Wereley N M 2009 Experimental characterization and static modeling of McKibben actuators *J. Mech. Des.* **131** 0910101–1010
[24] Tsagarakis N and Caldwell D G 2000 Improved modelling and assessment of pneumatic muscle actuators *Proc. IEEE Int. Conf. on Robotics and Automation* vol 4 pp 3641–6
[25] Zang K, Wang Y, Fu X and Hu X 2008 Study on modeling of McKibben pneumatic artificial muscle *Proc. Int. Conf. on Intelligent Computation Technology and Automation, ICICTA 2008* vol 1 pp 721–5
[26] Nakanishi D, Sugimoto Y, Honda H and Osuka K 2016 Experiments and analysis for modeling of McKibben pneumatic actuator *J. Robot. Mechatronics* **28** 830–6
[27] Bishop-Moser J and Kota S 2015 Design and modeling of generalized fiber-reinforced pneumatic soft actuators *IEEE Trans. Robot.* **31** 536–45
[28] Bishop-Moser J, Krishnan G and Kota S 2013 Force and moment generation of fiber-reinforced pneumatic soft actuators *IEEE Int. Conf. on Intelligent Robots and Systems* pp 4460–5
[29] Davis S, Tsagarakis N, Canderle J and Caldwell D G 2003 Enhanced modelling and performance in braided pneumatic muscle actuators *Int. J. Robot. Res.* **22** 213–27
[30] Shen W and Shi G L 2011 An enhanced static mathematical model of braided fibre-reinforced pneumatic artificial muscles *Proc. Inst. Mech. Eng. I* **225** 212–25
[31] Sanchez A, Mahout V and Tondu B 1998 Nonlinear parametric identification of a McKibben artificial pneumatic muscle using flatness property of the system *IEEE Conf. on Control Applications Proc.* vol 1 pp 70–74
[32] Tang R and Liu D 2012 An enhanced dynamic model for McKibben pneumatic muscle actuators *Australasian Conf. on Robotics and Automation, ACRA*
[33] Soleymani R and Khajehsaeid H 2020 A mechanical model for McKibben pneumatic artificial muscles based on limiting chain extensibility and 3D application of the network alteration theories *Int. J. Solids Struct.* **202** 620–30
[34] Chou C-P and Hannaford B 1994 Static and dynamic characteristics of McKibben pneumatic artificial muscles *Proc. IEEE Int. Conf. on Robotics and Automation* pp 281–6
[35] Chen D and Ushijima K 2014 Prediction of the mechanical performance of McKibben artificial muscle actuator *Int. J. Mech. Sci.* **78** 183–92
[36] Hoque M A, Petersen E and Fang X 2023 Effect of material properties on fiber-shaped pneumatic actuators performance *Actuators* **12** 129
[37] Kumar D, Ghosh S, Roy S and Santapuri S 2021 Modeling and analysis of an electro-pneumatic braided muscle actuator *J. Intell. Mater. Syst. Struct.* **32** 399–409
[38] Kurumaya S, Nabae H, Endo G and Suzumori K 2017 Design of thin McKibben muscle and multifilament structure *Sens. Actuators A* **261** 66–74
[39] Davis S and Caldwell D G 2006 Braid effects on contractile range and friction modeling in pneumatic muscle actuators *Int. J. Robot. Res.* **25** 359–69
[40] Klute G K and Hannaford B 1998 Fatigue characteristics of McKibben artificial muscle actuators *IEEE Int. Conf. on Intelligent Robots and Systems* vol 3 pp 1776–81
[41] Salahuddin B, Warren H and Spinks G M 2021 A comprehensive test method for measuring actuation performance of McKibben artificial muscles *Smart Mater. Struct.* **30** 045016
[42] Zhang Q, Beale D, Adanur S, Broughton R M and Walker R P 1997 Structural analysis of a two-dimensional braided fabric *J. Text. Inst.* **88** 41–52
[43] Quaglierini J, Arroyo M and Desimone A 2023 Mechanics of tubular meshes made of helical fibers and application to modeling McKibben artificial muscles *2023 IEEE Int. Conf. on Soft Robotics, RoboSoft 2023* (https://doi.org/10.1109/RoboSoft55895.2023.10122020)
[44] Sangian D 2016 New types of McKibben artificial muscles
[45] Tondu B, Emirkhanian R, Mathé S and Ricard A 2009 A pH-activated artificial muscle using the McKibben-type braided structure *Sens. Actuators A* **150** 124–30
[46] Sangian D, Naficy S, Spinks G M and Tondu B 2015 The effect of geometry and material properties on the performance of a small hydraulic McKibben muscle system *Sens. Actuators A* **234** 150–7
[47] Liu W and Rahn C R 2003 Fiber-reinforced membrane models of McKibben actuators *J. Appl. Mech.* **70** 853–9
[48] Gentry M F and Wereley N M 2008 Effects of braid angle on pneumatic artificial muscle actuator performance *Smart Mater. Adapt. Struct. Intell. Syst.* **43321** 617–23

[49] Kurumaya S, Nabae H, Endo G and Suzumori K 2019 Active textile braided in three strands with thin McKibben muscle *Soft Robot.* **6** 250–62
[50] Nguyen P H and Zhang W 2020 Design and computational modeling of fabric soft pneumatic actuators for wearable assistive devices *Sci. Rep.* **10** 9638
[51] Connolly F, Walsh C J and Bertoldi K 2017 Automatic design of fiber-reinforced soft actuators for trajectory matching *Proc. Natl Acad. Sci. USA* **114** 51–56
[52] Krishnan S, Nagarajan T, Rani A M A and Rao T 2012 Silk pneumatic artificial muscle (SPAM) construction for biomedical engineering application *BEIAC 2012–2012 IEEE Business, Engineering and Industrial Applications Coll.* pp 302–6
[53] Tondu B 2012 Modelling of the McKibben artificial muscle: a review *J. Intell. Mater. Syst. Struct.* **23** 225–53
[54] Chambers J M and Wereley N M 2022 Analysis of pneumatic artificial muscles and the inelastic braid assumption *Actuators* **11** 219
[55] Sangian D, Foroughi J, Farajikhah S, Naficy S and Spinks G M 2017 A bladder-free, non-fluidic, conductive McKibben artificial muscle operated electro-thermally *Smart Mater. Struct.* **26** 015011
[56] Cavallaro P V, Smith M P, O'Donnell J D, Redington A and Warner E 2022 Soft artificial muscle actuators for undersea launch & recovery systems *ASME Int. Mechanical Engineering Congress and Exposition, Proc. (IMECE)* vol 9
[57] Ball E, Lin Y and Garcia E 2013 Characterization and modeling of geometric variations in McKibben pneumatic artificial muscles *Proc. SPIE* **8686** 868605
[58] Ball E and Garcia E 2016 Effects of bladder geometry in pneumatic artificial muscles *J. Med. Devices* **10** 041001
[59] Wang G, Wereley N M and Pillsbury T 2015 Non-linear quasi-static model of pneumatic artificial muscle actuators *J. Intell. Mater. Syst. Struct.* **26** 541–53
[60] Garbulinski J, Balasankula S C and Wereley N M 2021 Characterization and analysis of extensile fluidic artificial muscles *Actuators* **10** 1–26
[61] Kadowaki J, Sasaki D, Yase H and Kusaka R 2021 Improvement of McKibben type artificial rubber muscle model based on end shape deformation *2021 IEEE Int. Conf. on Mechatronics, ICM 2021* (https://doi.org/10.1109/ICM46511.2021.9385626)
[62] Klute G K, Czerniecki J M and Hannaford B 1999 McKibben artificial muscles: pneumatic actuators with biomechanical intelligence *IEEE/ASME Int. Conf. on Advanced Intelligent Mechatronics, AIM* pp 221–6
[63] Tondu B and Zagal S D 2006 McKibben artificial muscle can be adapted to be in accordance with the Hill skeletal muscle model *Proc. 1st IEEE/RAS-EMBS Int. Conf. on Biomedical Robotics and Biomechatronics, 2006, BioRob 2006* vol 2006 pp 714–20
[64] Tanaka S, Nabae H and Suzumori K 2023 Back-stretchable McKibben muscles: expanding the range of antagonistic muscle driven joints *IEEE Robot. Autom. Lett.* **8** 5331–7
[65] Kobayashi R, Tanaka S, Nabae H, Endo G and Suzumori K 2025 McKibben muscle with elastic thread embedded in parallel extending range of motion of muscle-driven robots *IEEE Robot. Autom. Lett.* **10** 2534–41
[66] Cho H S, Kim T H, Hong T H and Park Y-L 2020 Ratchet-integrated pneumatic actuator (RIPA): a large-stroke soft linear actuator inspired by sarcomere muscle contraction *Bioinsp. Biomim.* **15** 036011
[67] Kim S, Lee S R, Lee S, Lee D and Shin D 2022 Power-efficient soft pneumatic actuator using spring-frame collateral compression mechanism *Actuators* **11** 76
[68] Tian W, Wakimoto S, Yamaguchi D and Kanda T 2024 Fabrication process for twisting artificial muscles by utilizing braiding technology and water-soluble fibers *IEEE Robot. Autom. Lett.* **9** 3147–54
[69] Faudzi A A M, Razif M R M, Nordin I N A M, Suzumori K, Wakimoto S and Hirooka D 2012 Development of bending soft actuator with different braided angles *2012 IEEE/ASME Int. Conf. on Advanced Intelligent Mechatronics (AIM)* (IEEE) pp 1093–8
[70] Feifei Z, Dohta S, Akagi T and Matsushita H 2006 Development of a bending actuator using a rubber artificial muscle and its application to a robot hand *2006 SICE-ICASE Int. Joint Conf.* pp 381–4
[71] Cullinan M F, Bourke E, Kelly K and McGinn C 2017 A mckibben type sleeve pneumatic muscle and integrated mechanism for improved stroke length *J. Mech. Robot.* **9** 011013
[72] Iwata K, Suzumori K and Wakimoto S 2011 Development of contraction and extension artificial muscles with different braid angles and their application to stiffness changeable bending rubber mechanism by their combination *J. Robot. Mechatronics* **23** 582–8
[73] Julie L, Mouloud O and Emmanuel V P 2021 Concentric muscles-miniature pneumatic actuator with integrated channel for surgical instruments *GMM-Fachberichte* pp 105–8
[74] Olson G and Menguc Y 2018 Helically wound soft actuators for torsion control *2018 IEEE Int. Conf. on Soft Robotics, RoboSoft 2018* pp 214–21
[75] Nordin I, Faudzi A, Razif M, Natarajan E, Wakimoto S and Suzumori K 2014 Simulations of two patterns fiber weaves reinforced in rubber actuator *J. Teknol.* **69** 133–8
[76] Nordin I N A M, Wakimoto S and Suzumori K 2015 Simulations of fiber braided bending actuator: investigation on position of fiber layer placement and air chamber diameter *2015 10th Asian Control Conf. (ASCC)* (IEEE) pp 1–5
[77] Du H, Shao R, Xu X and Xiong W 2022 Design and validation of a pneumatic bending actuator *Proc. 2022 7th Int. Conf. on Automation, Control and Robotics Engineering, CACRE 2022* pp 121–5
[78] Xiang C, Guo J, Chen Y, Hao L and Davis S 2018 Development of a SMA-fishing-line-McKibben bending actuator *IEEE Access* **6** 27183–9
[79] Maeda S, Wakimoto S and Yahara S 2016 Proposal of pneumatic rubber muscles with shape-memory polymer reinforcement fibers realizing desirable motion *2016 IEEE Int. Conf. on Robotics and Biomimetics, ROBIO 2016* pp 1221–6
[80] Lathrop R, Ourak M, Deprest J and Poorten E V 2022 Concentric dual-chamber pneumatic Artificial Muscles: miniature actuators designed for use in minimally invasive surgical instruments *J. Med. Robot. Re.* **7** 2241007
[81] Tsukagoshi H, Terashima K and Takai Y 2018 A self-propelled catheter capable of generating travelling waves with steering function by mono-line drive *2018 IEEE Int. Conf. on Robotics and Automation (ICRA)* (IEEE) pp 38–43
[82] Zhang S, Gong D and Yu J 2022 Design of a multi-connection pneumatic artificial muscle *2022 12th Int. Conf. on CYBER Technology in Automation, Control, and Intelligent Systems, CYBER 2022* pp 301–6
[83] Bruder D and Wood R J 2022 The chain-link actuator: exploiting the bending stiffness of McKibben artificial muscles to achieve larger contraction ratios *IEEE Robot. Autom. Lett.* **7** 542–8
[84] Kim J Y, Mazzoleni N and Bryant M 2021 Free strain gradient reversal of a variable recruitment fluidic artificial muscle bundle *Proc. SPIE* **11586** 115860L
[85] Suzumori K, Wakimoto S, Miyoshi K and Iwata K 2013 Long bending rubber mechanism combined contracting and extending tluidic actuators *2013 IEEE/RSJ Int. Conf. on Intelligent Robots and Systems* (IEEE) pp 4454–9
[86] Bishop-Moser J, Krishnan G, Kim C and Kota S 2012 Design of soft robotic actuators using fluid-filled fiber-reinforced elastomeric enclosures in parallel combinations *IEEE Int. Conf. on Intelligent Robots and Systems* pp 4264–9 .
[87] Kawamura S, Sudani M, Deng M, Noge Y and Wakimoto S 2019 Modeling and system integration for a thin pneumatic rubber 3-DOF actuator *Actuators* **8** 32

[88] Toyama Y and Wakimoto S 2016 Development of a thin pneumatic rubber actuator generating 3-DOF motion *2016 IEEE Int. Conf. on Robotics and Biomimetics, ROBIO 2016* pp 1215–20

[89] Wakimoto S, Suzumori K and Takeda J 2011 Flexible artificial muscle by bundle of McKibben fiber actuators *IEEE/ASME Int. Conf. on Advanced Intelligent Mechatronics, AIM* pp 457–62

[90] Yuzaki M, Iwata K, Wakimoto S and Kanda T 2018 Development of a thin pneumatic rubber actuator generating 3DOF motion—design using FEM analysis and fabrication of the actuator *ACTUATOR 2018–16th Int. Conf. and Exhibition on New Actuators and Drive Systems, Conf. Proc.* pp 563–6

[91] Lathrop B, Ourak M and Poorten E V 2022 Miniature pneumatic artificial muscles for use in surgical devices *GMM-Fachberichte* pp 4–7

[92] Vocke R D, Kothera C S, Chaudhuri A, Woods B K S and Wereley N M 2012 Design and testing of a high-specific work actuator using miniature pneumatic artificial muscles *J. Intell. Mater. Syst. Struct.* **23** 365–78

[93] Koizumi S, Kurumaya S, Nabae H, Endo G and Suzumori K 2018 Braiding thin McKibben muscles to enhance their contracting abilities *IEEE Robot. Autom. Lett.* **3** 3240–6

[94] Koizumi S, Kurumaya S, Nabae H, Endo G and Suzumori K 2020 Recurrent braiding of thin McKibben muscles to overcome their limitation of contraction *Soft Robot.* **7** 251–8

[95] Kadir M R A, Faudzi A A M and Rahman M A A 2022 Performance evaluation for braided McKibben pneumatic actuators in telescopic nested structure *IEEE Robot. Autom. Lett.* **7** 10906–13

[96] Na G, Nabae H and Suzumori K 2023 Braided thin McKibben muscles for musculoskeletal robots *Sens. Actuators A* **357** 114381

[97] Abe T, Koizumi S, Nabae H, Endo G, Suzumori K, Sato N, Adachi M and Takamizawa F 2019 Fabrication of "18 weave" muscles and their application to soft power support suit for upper limbs using thin McKibben muscle *IEEE Robot. Autom. Lett.* **4** 2532–8

[98] Hiramitsu T, Suzumori K, Nabae H and Endo G 2019 Experimental evaluation of textile mechanisms made of artificial muscles *RoboSoft 2019–2019 IEEE Int. Conf. on Soft Robotics* pp 1–6

[99] Marshall R, Souppez J-B R G, Khan M, Viola I M, Nabae H, Suzumori K, Stokes A A and Giorgio-Serchi F 2023 Mechanical characterisation of woven pneumatic active textile *IEEE Robot. Autom. Lett.* **8** 2804–11

[100] Funabora Y 2017 Prototype of a fabric actuator with multiple thin artificial muscles for wearable assistive devices *SII 2017–2017 IEEE/SICE Int. Symp. on System Integration* pp 356–61

[101] Funabora Y 2018 Flexible fabric actuator realizing 3D movements like human body surface for wearable devices *IEEE Int. Conf. on Intelligent Robots and Systems* pp 6992–7

[102] Nakagawa K, Sakai Y, Funabora Y and Doki S 2022 Turning a functional cloth into an actuator by combining thread-like thin artificial muscles and embroidery techniques *IEEE Robot. Autom. Lett.* **7** 5827–33

[103] Duan E and Bryant M 2022 Implications of spatially constrained bipennate topology on fluidic artificial muscle bundle actuation *Actuators* **11** 82

[104] Azizi E and Roberts T J 2013 Variable gearing in a biologically inspired pneumatic actuator array *Bioinsp. Biomim.* **8** 026002

[105] Wang Y, Liu C, Ren L and Ren L 2022 Bioinspired soft actuators with highly ordered skeletal muscle structures *Bio-Des. Manuf.* **5** 174–88

[106] Hiramitsu T, Suzumori K, Nabae H and Endo G 2023 Active textile: woven-cloth-like mechanisms consist of thin McKibben actuators *Adv. Robot.* **37** 480–94

[107] Kurumaya S, Suzumori K, Nabae H and Wakimoto S 2016 Musculoskeletal lower-limb robot driven by multifilament muscles *ROBOMECH J.* **3** 18

[108] Jenkins T and Bryant M 2020 Pennate actuators: force, contraction and stiffness *Bioinsp. Biomim.* **15** 046005

[109] Erin O, Pol N, Valle L and Park Y-L 2016 Design of a bio-inspired pneumatic artificial muscle with self-contained sensing *2016 38th Annual Int. Conf. of the IEEE Engineering in Medicine and Biology Society (EMBC)* (IEEE) pp 2115–9

[110] Felt W, Chin K Y and Remy C D 2016 Contraction sensing with smart braid McKibben muscles *IEEE ASME Trans. Mechatronics* **21** 1201–9

[111] Hagihara H, Wakimoto S, Kanda T and Furukawa S 2019 Operation of a pneumatic soft manipulator using a wearable interface with flexible strain sensors *IEEE Int. Conf. on Intelligent Robots and Systems* pp 4949–54

[112] Ho V A and Hirai S 2015 Measuring McKibben actuator shrinkage using fiber sensor *Proc. IEEE Int. Workshop on Robot and Human Interactive Communication* pp 628–33

[113] Kanno R, Watanabe S, Shimizu K and Shintake J 2021 Self-sensing McKibben artificial muscles embedded with dielectric elastomer sensor *IEEE Robot. Autom. Lett.* **6** 6274–80

[114] Legrand J, Loenders B, Vos A, Schoevaerdts L and Vander Poorten E 2020 Integrated capacitance sensing for miniature artificial muscle actuators *IEEE Sens. J.* **20** 1363–72

[115] Maselli M, Zrinscak D, Magliola V and Cianchetti M 2019 A piezoresistive flexible sensor to detect soft actuator deformation *RoboSoft 2019–2019 IEEE Int. Conf. on Soft Robotics* pp 372–7

[116] Misumi J, Wakimoto S and Suzumori K 2015 Experimental investigation of conductive fibers for a smart pneumatic artificial muscle *2015 IEEE Int. Conf. on Robotics and Biomimetics, IEEE-ROBIO 2015* pp 2335–40

[117] Omura K, Goto K, Wakimoto S and Kanda T 2018 Development of pneumatic valves and a fiber sensor for a smart artificial muscle *ACTUATOR 2018–16th Int. Conf. and Exhibition on New Actuators and Drive Systems, Conf. Proc.* pp 567–70

[118] Tian W, Wakimoto S, Kanda T and Yamaguchi D 2022 Displacement sensing of an active string actuator using a step-index multimode optical fiber sensor† *Sensors* **22** 3232

[119] Wakimoto S, Kogawa S, Matsuda H, Nagaoka K and Kanda T 2021 Comparison of smart artificial muscles with different functional fibers *GMM-Fachberichte* pp 124–6

[120] Wakimoto S, Misumi J and Suzumori K 2016 New concept and fundamental experiments of a smart pneumatic artificial muscle with a conductive fiber *Sens. Actuators A* **250** 48–54

[121] Wakimoto S, Suzumori K, Kanda T and Kure K 2007 Soft pressure sensor embedded in McKibben actuator *IEEE/ASME Int. Conf. on Advanced Intelligent Mechatronics, AIM* (https://doi.org/10.1109/AIM.2007.4412443)

[122] Yoshimoto Y, Wakimoto S, Tian W, Inoue K, Yamaguchi D and Kanda T 2022 Combination process of a pneumatic artificial muscle and a fiber optical sensor system † *Eng. Proceed.* **27** 86

[123] Zhong S, Gai Z, Yang Y, Zhao Y, Qi Y, Yang Y and Peng Y 2022 A contraction length feedback method for the McKibben pneumatic artificial muscle *Sens. Actuators A* **334** 113321

[124] Hitzmann A, Wang Y, Kessler T and Hosoda K 2021 Using conductive fabrics as inflation sensors for pneumatic artificial muscles *Adv. Robot.* **35** 995–1011

[125] Felt W and Remy C D 2014 Smart braid: air muscles that measure force and displacement *2014 IEEE/RSJ Int. Conf. on Intelligent Robots and Systems* (IEEE) pp 2821–6

[126] Wakimoto S, Suzumori K and Kanda T 2005 Development of intelligent McKibben actuator *2005 IEEE/RSJ Int. Conf. on Intelligent Robots and Systems, IROS* pp 487–92

[127] Kuriyama S, Ding M, Kurita Y, Ueda J and Ogasawara T 2009 Flexible sensor for McKibben pneumatic Artificial Muscle actuator *Int. J. Autom. Tech.* **3** 731–40

[128] Hamamoto I, Akagi T, Dohta S and Matsushita H 2006 Development of a flexible displacement sensor using nylon string coated with carbon and its application for McKibben actuator *2006 SICE-ICASE Int. Joint Conf.* pp 1943–6

[129] Antonelli M G, Zobel P B, De Marcellis A and Palange E 2022 Design and characterization of a Mckibben pneumatic muscle prototype with an embedded capacitive length transducer *Machines* **10** 1156

[130] Akagi T, Dohta S, Kenmotsu Y, Zhao F and Yoneda M 2012 Development of smart inner diameter sensor for position control of Mckibben artificial muscle *Proc. Eng.* **41** 105–12

[131] Goulbourne N C and Son S 2008 Numerical and experimental analysis of McKibben actuators and dielectric elastomer sensors *ASME Int. Mechanical Engineering Congress and Exposition, Proc.* vol 10 pp 175–86

[132] Goulbourne N C 2009 A mathematical model for cylindrical, fiber reinforced electro-pneumatic actuators *Int. J. Solids Struct.* **46** 1043–52

[133] Yahara S, Wakimoto S, Kanda T and Matsushita K 2019 McKibben artificial muscle realizing variable contraction characteristics using helical shape-memory polymer fibers *Sens. Actuators A* **295** 637–42

[134] Takashima K, Rossiter J and Mukai T 2010 McKibben artificial muscle using shape-memory polymer *Sens. Actuators A* **164** 116–24

[135] Lopez-Diaz A *et al* 2020 Autonomous self-healing pneumatic McKibben muscle based on a new hydrogel material *2020 3rd IEEE Int. Conf. on Soft Robotics, RoboSoft 2020* pp 13–18

[136] Sangian D, Jeiranikhameneh A, Naficy S, Beirne S and Spinks G M 2019 Three-dimensional printed braided sleeves for manufacturing mckibben artificial muscles *3D Print. Addit. Manuf.* **6** 57–62

[137] Ball E J, Meller M A, Chipka J B and Garcia E 2016 Modeling and testing of a knitted-sleeve fluidic artificial muscle *Smart Mater. Struct.* **25** 115024

[138] Bennington M J, Wang T, Yin J, Bergbreiter S, Majidi C and Webster-Wood V A 2023 Design and characterization of viscoelastic McKibben actuators with tunable force-velocity curves *2023 IEEE Int. Conf. on Soft Robotics, RoboSoft 2023* (https://doi.org/10.1109/RoboSoft55895.2023.10122014)

[139] Naclerio N D and Hawkes E W 2020 Simple, low-hysteresis, foldable, fabric pneumatic artificial muscle *IEEE Robot. Autom. Lett.* **5** 3406–13

[140] Risangtuni A G, Suprijanto S and Nazaruddin Y Y 2021 Markerless video motion analysis of a modified McKibben muscle soft pneumatic actuator *Proc. 2021 Int. Conf. on Instrumentation, Control, and Automation, ICA 2021* pp 28–32

[141] Salahuddin B, Warren H and Spinks G M 2020 Thermally actuated hydrogel bead based braided artificial muscle *Smart Mater. Struct.* **29** 055042

[142] Nabae H, Kodaira A, Horiuchi T, Asaka K, Endo G and Suzumori K 2019 Soft polymer-electrolyte-fuel-cell tube realizing air-hose-free thin McKibben muscles *IEEE Int. Conf. on Intelligent Robots and Systems* pp 8287–93

[143] Kodaira A, Nabae H, Horiuchi T, Asaka K, Endo G and Suzumori K 2021 Au/Pt double-layer electrodes and expanding internal chamber for improving air-hose-free thin McKibben muscles *2021 IEEE 4th Int. Conf. on Soft Robotics, RoboSoft 2021* pp 419–26

[144] Vial D, Tondu B, Lopez P, Aurelle Y and Ricard A 1996 Ion-exchange polymer artificial muscle and actuating system *Proc. SPIE* 2779 359–64

[145] Mirvakili S M, Sim D, Hunter I W and Langer R 2020 Actuation of untethered pneumatic artificial muscles and soft robots using magnetically induced liquid-to-gas phase transitions *Sci. Robot.* **5** aaz4239

[146] Cacucciolo V, Nabae H, Suzumori K and Shea H 2020 Electrically-driven soft fluidic actuators combining stretchable pumps with thin McKibben muscles *Front. Rob. AI* **6** 146

[147] Zhagiparova A, Golubev V and Kim D 2025 Recent developments in pneumatic artificial muscle actuators *Actuators* **14** 582

[148] Zhang X and Krishnan G 2018 A nested pneumatic muscle arrangement for amplified stroke and force behavior *J. Intell. Mater. Syst. Struct.* **29** 1139–56

[149] Satheeshbabu S, Thompson N, Xiao C and Krishnan G 2019 Architectures of soft pneumatic actuators inspired by muscle fiber arrangements *2019 2nd IEEE Int. Conf. on Soft Robotics (Robosoft)* (IEEE) pp 271–6

[150] Shi M and Yeatman E M 2021 A comparative review of artificial muscles for microsystem applications *Microsyst. Nanoeng.* **7** 95